Lehrstuhl für
Technische Dynamik
Prof. Dr.-Ing. habil. Sigrid Leyendecker

Report
Institute of Applied Dynamics
2021

Friedrich-Alexander-Universität
Technische Fakultät

Prof. Dr.-Ing. habil. S. Leyendecker
Lehrstuhl für Technische Dynamik
Friedrich-Alexander-Universität Erlangen-Nürnberg
Immerwahrstrasse 1
91058 Erlangen
Tel.: 09131 8561000
Fax.: 09131 8561011
www: `https://www.ltd.tf.fau.de`

Editors: E. Fleischmann, D. Phansalkar

Contents

1 Preface

This report gives a summary of the scientific and teaching activities of the Institute of Applied Dynamics (LTD) at the Friedrich-Alexander-Universität Erlangen-Nürnberg during the year 2020. The members of LTD are passionately working on topics such as multibody dynamics and robotics, motion capturing, biomechanics, structure preserving methods and optimal control.
Many thanks to our technical, scientific and admin staff at LTD and also to all the students involved to make it a successful year at the Institute of Applied Dynamics. We wish you an enjoyable time glancing through our annual report.

2 Team

head of institute
Prof. Dr.-Ing. habil. Sigrid Leyendecker

technical staff
Beate Hegen
M.Sc. Elisa Fleischmann
M.Sc. Markus Lohmayer

academic scientist

Dr. rer. nat. Holger Lang, Akad. Rat	until 30.06.2021
M.Sc. Giuseppe Capobianco, Akad. Rat	from 01.12.2021

postdoc
Dr. Rodrigo Sato Martín de Almagro
Dr.-Ing. Dengpeng Huang

scientific staff

M.Sc.hons. Xiyu Chen	
M.Sc. Birte Coppers	from 01.10.2021
M.Sc. Simon Heinrich	from 01.11.2021
M.Sc. David Holz	
M.Sc. Michael Klebl	until 31.03.2021
M.Sc. Denisa Martonová	
M.Sc. Johann Penner	until 30.09.2021
M.Sc. Dhananjay Phansalkar	
M.Sc. Uday Phutane	until 30.09.2021
M.Sc. Eduard Sebastian Scheiterer	
M.Sc. Matthias Schubert	from 01.10.2021
M.Sc. Martina Stavole	
M.Sc. Theresa Wenger	

students

Johannes Bayer	Dorothea Brackenhammer	Xiaojing Chen
Patrick Deferner	Lou Ebert	Jakob Fischer
Jonas Fischer	Marc Gadinger	Alexander Greiner
Maximilian Hausch	Simon Heinrich	Elena Hobbacher
Daphne Hohbohm	Xuyue Huang	Anne Kirsch
Zandantsetseg Khishigdulam	Anne Kirsch	Julian Lang
Xihao Liu	Markus Menzel	Christoph Mölter
Claude J.I. Motsebo Fotso	Manuel Ott	Felix Pfister
Arne Pietsch	Nivashini Radhakrishnan	Isabella Reiher
Julian Reiner	Benjamin Schoder	Matthias Schubert
Bastial Stühler	Aiswarya Uttla	Nicolas Valbuena
Juliane Wunder	Mohammadhosein Zakaryapour	

Student assistants are mainly active as tutors for young students in basic and advanced lectures at the Bachelor and Master level. Their contribution to high quality teaching is indispensable, thus financial support from various funding sources is gratefully acknowledged.


G. Capobianco

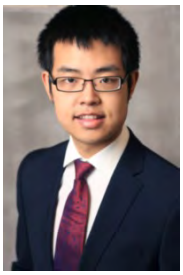
X. Chen


B. Coppers


E. Fleischmann


B. Hegen


S. Heinrich


D. Holz


D. Huang


M. Klebl


H. Lang

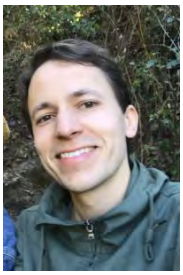
M. Lohmayer


D. Martonová


J. Penner


D. Phansalkar


U. Phutane


R.T. Sato


E.S. Scheiterer


M. Schubert


M. Stavole


T. Wenger


S. Leyendecker

3 Research

3.1 ETN – THREAD

The Institute of Applied Dynamics takes part in the ETN (European Training Network) project "Joint Training on Numerical Modelling of Highly Flexible Structures for Industrial Applications – THREAD" funded by the European Commission's Marie Skłodowska Curie Programme which is part of Horizon 2020. The project is coordinated by Prof. Dr. Martin Arnold from the Institute of Mathematics at the Martin Luther University Halle-Wittenberg (MLU). Prof. Dr.-Ing. habil. Sigrid Leyendecker is principal investigator and work package leader and M.Sc. Martina Stavole participates as early stage researcher (ESR10) since 2020.
THREAD addresses the mechanical modelling, mathematical formulations and numerical methods for highly flexible slender structures like yarns, cables, hoses or ropes that are essential parts of high-performance engineering systems. The complex response of such structures in real operational conditions is far beyond the capabilities of current virtual prototyping tools.
This year the first deliverables of the three main work packages have been successfully submitted. And many project activities, i.e. network-wide training events, conferences and secondments, took place on-site. Also, the project had a successful second annual meeting on 5-7 October 2021 in Seville, Spain.

M.Sc. Martina Stavole, successfully completed a three months industrial secondment at Karl Storz in Taillin, Estonia. The aim of the internship was to study the stiffness parameters of endoscopes for modelling purposes through an experimental campaign carried out on several endoscopes.

3.2 FRASCAL – Fracture across Scales

The DFG research training group FRASCAL – Fracture across Scales (GRK 2423) led by Prof. Dr.-Ing. habil. Paul Steinmann from the Institute of Applied Mechanics at FAU Erlangen-Nürnberg has successfully continued to pursue its research goals. The Institute of Applied Dynamics takes part within FRASCAL P9 project – Adaptive Dynamic Fracture Simulation. The project is supervised by Prof. Dr.-Ing. habil. Sigrid Leyendecker and carried out by M.Sc. Dhananjay Phansalkar. It aims to develop robust and efficient numerical techniques to investigate kinetics of fracture mechanics. It will develop adaptive strategies to obtain suitable combinations of spatial and temporal mesh. These methods are developed in close cooperation with RTG's Mercator fellow Prof. Dr. Michael Ortiz and Prof. Dr.-Ing. PD Kerstin Weinberg from Universität Siegen. The first FRASCAL Virtual Colloquium took place weekly from March 12nd to July 22nd, 2021, providing a platform to discuss recent advances in the computational modeling of fracture at various length and time scales. Between October 14 and 15, 2020 the members of FRASCAL met at Hotel Riesengebirge, Neuhof an der Zenn for a RTG seminar. It sparked off discussions between doctoral candidates and principal advisors from various

projects for possible collaboration. Towards the end of the year, on November 26, 2021 principal advisors shared their perspective on fracture in the 1st virtual FRASCAL symposium.

Image by: Andrea Dakkouri-Baldauf

3.3 SPP 1886

The German Research Foundation (DFG) Priority Programme "Polymorphic uncertainty modelling for the numerical design of structures – SPP 1886" is coordinated by Professor Dr.-Ing. Michael Kaliske from Technische Universität Dresden and Prof. Dr.-Ing. habil. Sigrid Leyendecker is part of the programme committee and principal investigator of one of the projects. In 2021, the Institute of Applied Dynamics successfully took part in the online winter school organized by the SPP and presented the progress in the research of dynamic analysis of prosthetic structures with polymorphic uncertainty in the annual meeting in October.

3.4 DFG dielectric elastomer project

The DFG-Einzelförderung / Sachbeihilfe "Electromechanically coupled beam models for stacked dielectric elastomer actuators" project, initiated last year with Prof. Dr.-Ing. habil. Sigrid Leyendecker as project leader and fellow Dr.-Ing. Dengpeng Huang in the research front. Stacked dielectric elastomer actuators bear analogy to the behaviour of human muscles in terms of contracting in length direction when actuated. They are suitable for point-by-point application of a force. Therefore, dielectric elastomers allow for a sophisticated, efficient and noiseless actuation of systems. However, the use of elastic actuators is also accompanied by new control challenges. As the computational cost for solving optimal control problems is significantly affected by the number of model degrees of freedom, reduced and problem specific actuator models are superior to general but cost-intensive finite element models. To this end, a beam model has been developed in this project for the stacked dielectric elastomer actuators, which has been published in the Journal of Computational Mechanics recently. The application of the beam model in complex multibody system is ongoing.

3.5 Heart project

The heart project is focusing on the modelling of the cardiac function to better understand cardiovascular disease, to be able to early detect or even predict heart failure and develop adequate patient specific therapies and medical devices. We are currently working on a rat as well as a human heart model. The former is related to the rat heart project, which is an established research cooperation between the Institute of Applied Dynamics, the Pediatric Cardiology and the Institute of Medical Biotechnology at Friedrich-Alexander-Universität Erlangen-Nürnberg and is funded by the Klaus Tschira Stiftung. The goal of the project is to explore the heart function under pathological and normal conditions by developing a computational model of a rat heart which will be validated with experiments at the

Pediatric Cardiology and the Institute of Medical Biotechnology. In 2021, we were mainly focusing on the smoothed finite element method in modelling and simulation of active cardiac mechanics as well as on the development of a a transmural path model to compute the orthotropic tissue structure in heart simulations.

3.6 Characterisation of Macromolecules

The characterisation of macromolecules project is a cooperation research between the Institute of Applied Dynamics at Friedrich-Alexander-Universität Erlangen-Nürnberg and UCSF Department of Bioengineering and Therapeutic Sciences and is funded by German Research Foundation (DFG). The purpose of this project is characterizing macromolecules e.g. SARS CoV-2 main protease by using the kino-geometric sampling (KGS) method. The rigidity and conformation transition analysis of SARS CoV-2 main protease mutation, will benefit drug development in the SARS CoV-2 field. The project is cooperated by Dr. Henry van den Bedem from Stanford University. M.Sc. Xiyu Chen is focusing on the rigidity analysis and the mutation analysis for SARS CoV-2 main protease binding with different ligands by using the KGS method.

3.7 SFB 1483 – EmpkinS

Developing sensor technology and collecting movement data of the human body is the aim of the new Collaborative Research Center SFB 1483, which has just been approved by the German Research Foundation (DFG). The new SFB bears the project title “Empatho-Kinaesthetic Sensor Technology” (EmpkinS). His research aims to combine the external observation of body movements, such as movements of the head, torso and limbs, facial expressions or even a slight twitch under the surface of the skin with internal processes using body function models. The research team headed by Prof. Dr. Martin Vossiek from the Institute of Microwaves and Photonics and Prof. Dr. Björn Eskofier from the Machine Learning and Data Analytics Lab wants to achieve this by developing methods and technologies that link information from external movements with internal biomedical processes. The external movements are measured with sensory systems, which are also developed within the CRC. The aim of EmpkinS is to enable the simultaneous detection of several body (dys) functions with non-invasive and in the future easily available sensors. The focus of EmpkinS is on medical issues in immunology, neurology and palliative medicine as well as mental illnesses such as depression and stress.
Subproject C04 “Analysis of Degenerative Movement Restrictions by Embedding Empathokinesthetic Sensor Data in Biomechanical Human Models” is located at the Institute of Applied Dynamics with principal investigator Prof. Dr.-Ing. habil. Sigrid Leyendecker and M.Sc. Simon Heinrich joined in November as doctoral candidate.
In close collaboration with the Institute of Applied Dynamics the subproject D01 “Movement Patterns in Hand Motion from Empathokinesthetic Sensor Data as a Diagnostic Parameter for Disease Activity in Patients with Rheumatic Disease” located at the Department of Internal Medicine 3 – Rheumatology and Immunology started in September. Dr. sport science Anna-Maria Liphardt is working as principal investigator in this project and M.Sc. Birte Coppers as doctoral candidate.
The project had a successful kickoff on October 26, 2021 in Fürth, Germany.

3.8 Scientific reports

The subsequent pages present a brief overview on the current research projects pursued at the Institute of Applied Dynamics. These are partly financed by third-party funding German Research Foundation (DFG), the Klaus Tschira Stiftung, the Federal Ministry of Education and Research (BMBF) the European Training Network (ETN) and in addition by the core support of the university.

Research topics

SARS CoV-2 Main Protease Mutation Analysis By The Kinematic Method
Xiyu Chen, Sigrid Leyendecker, Henry van den Bedem

Movement Patterns in Hand Motion from Empathokinesthetic Sensor Data as a Diagnostic Parameter for Disease Activity in Patients with Rheumatic Disease
Birte Coppers, Sara Bayat, Arnd Kleyer, Georg Schett, Simon Heinrich, Sigrid Leyendecker, Anna-Maria Liphardt

Comparison of different approaches for the personalization of a kinematic hand model
Simon Heinrich, Birte Coppers, Anna-Maria Liphardt, Sigrid Leyendecker

A transmural path model to compute the orthotropic tissue structure in heart simulations
David Holz, Minh Tuan Duong, Denisa Martonová, Muhannad Alkassar and Sigrid Leyendecker

Electromechanically coupled beam models for stacked dielectric elastomer actuators
Dengpeng Huang, Sigrid Leyendecker

First steps towards a cardiac assist device to support a diseased rat heart
Denisa Martonová, Dorothea Brackenhammer, David Holz, Maximilian Landgraf, Muhannad Alkassar and Sigrid Leyendecker

CyberGlove for Clinical Use
Johannes Michaelis, Isabella Reiher, Simon Heinrich, Birte Coppers, Anna-Maria Liphardt, Sigrid Leyendecker

Dynamic phase-field model for the brittle fracture
Dhananjay Phansalkar, Michael Ortiz, Kerstin Weinberg, Sigrid Leyendecker

Several topics on variational integrators
Rodrigo T. Sato Martín de Almagro, Sigrid Leyendecker

Forward dynamics simulation of a human leg with a carbon spring prosthetic foot
Eduard S. Scheiterer, Sigrid Leyendecker

Optimal control of a geometrically exact beam
Matthias Schubert, Sigrid Leyendecker

Homogenized constitutive properties of multi-layered beam cross-sections
Martina Stavole, Sigrid Leyendecker

Analysis of multirate variational integrators and mixed order variational integrators by Modulated Fourier expansions
Theresa Wenger, Sina Ober-Blöbaum and Sigrid Leyendecker

SARS CoV-2 main protease mutation analysis by the kinematic method

Xiyu Chen, Sigrid Leyendecker, Henry van den Bedem[1] [2]

Protein flexibility is a significant factor for protein conformation, and the ligand binding with protein modifies its flexibility. In general, the larger flexibility causes more complex protein conformational properties and activity. Since 2019, the new coronavirus SARS CoV-2 has caused pandemics. The main protease (Mpro) of SARS CoV-2 is known as one of the potential drug targets whose investigation is worthwhile for potential drug development. In particular, Mpro selecting as a target is relatively safe because it has no human homolog, which decreases the probability to target a wrong host protein [1, 2]. The SARS CoV-2 plays an important role in the processing of the coronavirus replicase polyprotein and cut the polyprotein into individual protein. It includes three domains in the Mpro protomer and the N-terminal finger (1-9) normally has a significant influence on its activity [3]. However, the influence of the Mpro monomer mutations are still not clear. In this work, we investigated the mutation effects of the Mpro of the new Sars coronavirus based on our kinematic flexibility analysis, which can analyze larger molecules and needs less computational costs.

Kinematic flexibility analysis (KFA) is an efficient, fast method to analyze the conformational flexibility and transition of 3D macromolecules and a helpful tool to investigate how their flexibility influences their function. Kinematically, hydrogen bonds and hydrophobic interactions can be modeled as holonomic constraint. KFA treats all covalent bond (dihedral angles) as degrees of freedom $\mathbf{q}$ and the non-covalent interaction as holonomic constraints $\mathbf{\Phi}(\mathbf{q})=\mathbf{0}$, see [4, 5, 6]. Consistent with these holonomic constraints, the velocity constraints read

$$\frac{d\mathbf{\Phi}}{dt} = \mathbf{J}\dot{\mathbf{q}} = \mathbf{0}$$

Through singular value decomposition of the Jacobian matrix J, a basis for its nullspace can be determined. This nullspace is identical to the current conformation tangent space. The nullspace contains the addmissible velocities $\dot{\mathbf{q}}$ and it provides the required information for the molecular rigidity analysis and for conformational transitions.

O. S. Amamuddy et al. [1] studied Sars Mpro conformation and estimated possible mutation position. Based on these mutation positions, we apply the kinematic transition method to analyze the change in flexibility after the mutation. These mutation positions are: A7, G15, M17, V20, T45, D48, M49, R60, K61, A70, G71, L89, K90, P99, Y101, R105, P108, A116, A129, P132, T135, I136, N151, V157, C160, A173, P184, T190, A191, A193, T196, T198, T201, L220, L232, A234, K236, Y237, D248, A255, T259, A260, V261, A266, N274, R279 and S301L. Different inhibitor ligands and different mutations are investigated in this work with regard to their ability to influence the flexiblity of the SARS CoV-2 Mpro. The pdbfile 6Y2E is Mpro without ligand binding and the other pdbfiles is Mpro with one ligand. The root mean squared fluctuation (RMSF) of the atom positions is a good indicator for the flexiblity, which influence the activity and conformational property of Mpro. Fig. 1(A) shows the ratio between the root mean squared fluctuation (RMSF) values of Mpro with ligands and without ligands. Most of the RMSF ratios are less than 1 which means that the binding of Mpro with the ligand cause the RMSF value to decrease. This indicates that the Mpro becomes more rigidified when binding with the ligand. In particular for the domain I and domain II, the pdbfile 6LU7 with inhibitor N3 shows a large decrease of the RMSF value. Fig. 1(B) shows the RMSF ratios between Mpro with mutation

[1]Atomwise, Inc. 717 Market Street, San Francisco, CA 94103 USA
[2]Department of Bioengineering and Therapeutic Sciences, UCSF, California, USA

and without mutation. The mutation position is marked in the figure. The pdbfile 6LU7 shows a substantial increase in the RMSF value after mutation. The pdbfile 5R81 shows largely increased RMSF values in the domain III. Also around the mutation positions, the RMSF values increase largely. Furthermore, the pdbfile 5R80 and 6Y2F show decreased RMSF values after the mutation in the domain I and II. In the future, we can apply this rigidity analysis for the dtug development of the SARS CoV-2.

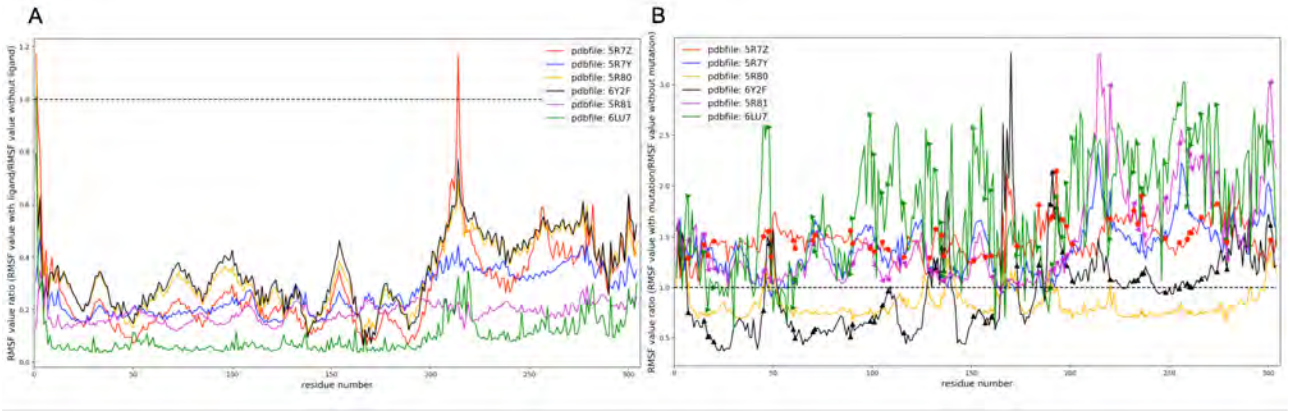

Figure 1: Coronavirus SARS CoV-2 Mpro mutation analysis based on the kinematical method. (A) the RMSF value ratio between with ligand and without ligand for different pdbfile. (pdb: 5R7Z, 5R7Y, 5R80, 6Y2F, 5R81 and 6LU7, Mpro with ligand binding) (B) the RMSF value ratio between Mpro mutation and without mutation for different pdbfile. The positions of the residues which undergoing mutations are highlighted by the marker

References

[1] O. S. Amamuddy, Gennady M. Verkhivker and Ö. T. Bishop. Impact of emerging mutations on the dynamic properties the SARS-CoV-2 main protease: an in silico investigation. Journal of Chemical Information and Modeling. 2021

[2] S. Chen et al. Mutation of Gly-11 on the Dimer Interface Results in the Complete Crystallographic Dimer Dissociation of Severe Acute Respiratory Syndrome Coronavirus 3C-like Protease. Journal of Biological Chemistry. 283, 554-564, 2008

[3] Kneller, D.W., Phillips, G., O. Neill, H.M. et al. Structural plasticity of SARS-CoV-2 3CL Mpro active site cavity revealed by room temperature X-ray crystallography. Nat Commun 11, 3202, 2020

[4] D. Budday, S. Leyendecker, and H. van den Bedem. Kinematic Flexibility Analysis: Hydrogen Bonding Patterns Impart a Spatial Hierarchy of Protein Motion. Journal of Chemical Information and Modeling 58(10), 2108-2122, 2018

[5] D. Budday, S. Leyendecker, and H. van den Bedem. Geometric analysis characterizes molecular rigidity in generic and non-generic protein configurations. Journal of the Mechanics and Physics of Solids 83, 36-47, 2015

[6] X. Chen, S. Leyendecker, H. van den Bedem. Kinematic Flexibility Analysis of Active and Inactive Kinase Conformations Proceedings in Applied Mathematics and Mechanics, 2020

Movement patterns in hand motion from empathokinesthetic sensor data as a diagnostic parameter for disease activity in patients with rheumatic disease

B. Coppers[1], S. Bayat[1], A. Kleyer[1], G. Schett[1], S. Heinrich, S. Leyendecker, A.M. Liphardt[1]

In the context of the recently initiated collaborative research center (CRC) Empathokinesthetic Sensory, (Empkins) SFB 1483 we are aiming to characterize hand movements in healthy individuals and patients with inflammatory arthritis. The goal is to identify objective functional parameters for monitoring disease activity in patients suffering from inflammatory-destructive joint diseases like rheumatoid arthritis (RA) and psoriasis arthritis (PsA). Recognizing early signs of inflammation at the onset of the disease is vital for effective medical treatment. The joints of the hand and fingers are most frequently affected at the early stage of the disease which leads to impaired hand function [1]. Currently, measuring disease activity in RA and PsA relies on a composite set of patient-reported and physician-assessed items combined with only one objective blood marker of inflammation [2]. The measurement of the functional status is based mainly on patient-reported data [3] and conventional clinical methods are lacking objectivity. An objective evaluation of the functional state of the hand for disease monitoring and prediction would therefore be desirable [4].

The study will assess demographic and disease specific clinical and disease activity data, currently used hand function tests, such as the Moberg-Pick-Up Test (MPUT) [5], hand function questionnaires (Michigan Hand Outcomes Questionnaire) and isometric handgrip strength. Tendon and joint structure will be quantified by ultrasound and HR-pQCT, muscle activity by Electromyography, and general physical activity using the International Physical Activity Questionnaire. Furthermore, simple hand movements will be captured with optoelectronic measurement systems (OMS) and radar [6]. Patient data will be compared to sex and age-matched healthy controls.

In preparation of the above described project, we conducted the EmpkinS Pilot Study [7]. Twenty-four RA patients (17 female, 7 male; 62.3 ± 9.1 years, VAS global 29.4 ± 25.8) and 23 healthy controls (12 f, 11 m; age: 50.2 ± 16.1 years) participated in this experiment [7],[8]. As an initial attempt, we adapted the performed MPUT using the data of the OMS for a detailed spatiotemporal analysis to compare hand function of patients with RA to that of healthy controls 1.

Figure 1: MPUT objects and hand marker setup

Transport time for each of the 12 MPUT objects was divided into a reaching phase (first touch to safe grip) and a manipulation phase (safe grip to drop) using the video recording or marker trajectories. First statistical analysis highlighted that the reaching phase of the MPUT and specific objects have

[1]Department of Internal Medicine 3 – Rheumatology and Immunology, University Clinic Erlangen, Friedrich-Alexander-Universität Erlangen-Nürnberg, Ulmenweg 18, D-91054 Erlangen, Germany

the potential to better discriminate RA from controls. The overall MPUT times were affected by age for both patients and healthy controls. This emphasizes the importance of a broad inclusion of patient and healthy participants to differentiate between different age groups and sexes as planned in the upcoming study.

Future steps will be to characterize hand movement parameters that can be adequately captured with EmpkinS hardware (OMS, radar) with the goal to allow a simple and objective assessment of hand function that is well related to disease status in inflammatory arthritis.

Acknowledgments
This work was supported by the German Research Foundation (DFG, German Research Foundation) under Grant SFB 1483 –Project-ID 442419336.

References

[1] Liphardt, A.M.; Manger, E.; Liehr, S.; Bieniek, L.; Kleyer, A.; Simon, D.; Tascilar, K.; Sticherling, M.; Rech, J.; Schett, G.; et al. (2020). *Similar impact of psoriatic arthritis and rheumatoid arthritis on objective and subjective parameters of hand function.* ACR Open Rheumatol. **2(12)**, 734–740(2020).

[2] Aletaha, D., et al . *Rheumatoid arthritis classification criteria: an American College of Rheumatology/European League Against Rheumatism collaborative initiative.* Arthritis Rheum. **62(9)**, 2569-81 (2010).

[3] Günay, S. M., et al. *Relationship between patient-reported and objective measurements of hand function in patients with rheumatoid arthritis.* Reumatismo. **68(4)**, 183-187 (2016).

[4] Bremander, A., et al. *Importance of Measuring Hand and Foot Function Over the Disease Course in Rheumatoid Arthritis: An Eight-Year Follow-Up Study.* Arthritis Care Res (Hoboken) **71(2)**, 166-172(2019).

[5] Ng, C. L., et al. *The Moberg pickup test: Results of testing with a standard protocol.* Journal of Hand Therapy. **12(4)**, 309-312(1999).

[6] Sancho-Bru, J. L. *Grasp modelling with a biomechanical model of the hand.* Computer Methods in Biomechanics and Biomedical Engineering **17(4)**, 297-310(2014).

[7] Phutane, U., Liphardt A.M., Bräunig J., et. al. *Evaluation of Optical and Radar Based Motion Capturing Technologies for Characterizing Hand Movement in Rheumatoid Arthritis-A Pilot Study.* Sensors (Basel) **21(4)**, 1208(2021).

[8] Phutane, U., et al. *Evaluation strategies for assessing finger motion in rheumatoid arthritis to estimate impaired hand function.* 28th Congress of the International Society of Biomechanics - ISB (Stockholm, 2021-07-25 - 2021-07-29).

Comparison of different approaches for the personalization of a kinematic hand model

Simon Heinrich, Birte Coppers, Anna-Maria Liphardt, Sigrid Leyendecker

Dynamic simulations of human hands can be used to get more information about forces, stresses and general loads in the human hand during everyday motions. One approach to simulate human hands is within the framework of optimal control optimizing a certain objective with the goal to create realistic movements. Measurements of hand movement can be used as a natural reference to mimic a persons' movement. However, it is necessary to personalize the hand model when using these measurements in simulations, since the motion is tracked via markers attached to the hand. For that the markers are also defined virtually on the hand model. If the real and the modeled hand are not similar and have not similarly placed markers, a similar trajectory for measured and virtual markers does not indicate a similar motion of the real hand and the biomechanical model.
Therefore, different approaches to define increasingly individualized hand models are compared by performing an inverse kinematics simulation of a simple movement and rating the result by the average deviation of measured and simulated marker trajectories. The measurements used here are taken from [1] where an optoelectronic measurement system with reflective markers in was used. The marker setup is shown in Figure 1(a). The markers on the thumb are not used in this work. As a reference the postuer as shown in Fig. 1(b) is used, named RP. Two different motions are considered, on is a flexion in the distal and proximal interphalangeal joints, called JOINT and the other one is a cylinder grasping motion with three objects of different size, called CYLINDER.

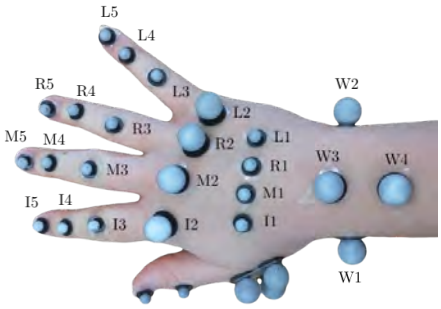

(a) Marker setup

(b) Reference posture

Figure 1: Marker setup with 29 markers in (a) and hand in reference posture (RP) in Figure (b). The 5 markers on the thumb are not used in this work. Both figures are taken from [1].

Kinematic hand models can be set up using rigid bodies connected by joints. The location and orientation of each body is described by the position vector of its center of mass and three orthonormal vectors, the so called directors [3]. The single bodies are connected by joints, using one degree of freedom revolute joints, two degrees of freedom universal joints and two degrees of freedom nino joints [4].
The most generic hand model is created by scaling the segment dimensions with relations that depend on hand length as in [2] and literature values. To further personalize the model, the markers in the RP measurement are used to calculate phalangeal segment lengths and the angles between the metacarpals. Additionally, a model can use individually calculated local marker coordinates with respect to the corresponding segment. These are also calculated from the RP measurement. The last hand model uses a constraint optimization in *Matlab* (The MathWorks Inc. Massachusetts) with `fmincon`. It is based on the idea that the joint centers have a constant distance from each other, the markers are fixed to one segment and rotate around a joint center with a fixed distance and the

flexion-extension is a quasi planar motion [5]. The minimization problem is stated in equation (1). The indices refer to the kth segment of the ith digit at timestep t. The variables in this optimization are the lengths between two joint centers $||\boldsymbol{L}_k^i||$, the distances from the marker to the adjacent joint center $||\boldsymbol{d}_k^i||$, the initial orientation of the vectors from marker to joint center $\boldsymbol{e}_k^i(t=1)$ and the incremental angles of rotation $\delta_k^i(t)$ for $\boldsymbol{e}_k^i(t)$ between two successive time steps. Further used quantities are the vector between two adjacent markers $\boldsymbol{l}_k^i(t)$ and the direction vectors from marker to joint center $\boldsymbol{e}_k^i(t)$.

$$
\begin{aligned}
\min_{||\boldsymbol{L}_k^i||,||\boldsymbol{d}_k^i||,\boldsymbol{e}_k^i(t=1),\delta_k^i(t)} \quad & \sum_{k=1}^{3}\sum_{t=1}^{T}\left(||\boldsymbol{L}_k^i|| - ||\boldsymbol{l}_k^i(t) + ||\boldsymbol{d}_k^i||\boldsymbol{e}_{k-1}^i(t) - ||\boldsymbol{d}_k^i||\boldsymbol{e}_k^i(t)||\right)^2 \\
\text{subject to} \quad & ||\boldsymbol{e}_k^i(t)|| = 1 \\
& \boldsymbol{e}_k^i(t) \quad \text{lies in plane} \\
& -\frac{\pi}{9} \leq \delta_k^i(t) \leq \frac{\pi}{9} \\
& ||\boldsymbol{L}_k^i|| \quad \text{within } 50\,\% - 150\,\% \text{ of literature values} \\
& ||\boldsymbol{d}_k^i|| \quad \text{within } 60\,\% - 160\,\% \text{ of literature values}
\end{aligned}
\tag{1}
$$

The different hand models are used in an inverse kinematic simulation with the JOINT measurement. The simulation is conducted with `fminunc` for unconstrained optimizations in *Matlab*. The optimization problem is stated in equation (2). Its value is also called the residual error. The index m is used for different markers on the model and t is used for the time steps. The variable is the incremental change in generalized coordinates $\Delta\boldsymbol{q}$. The measured marker locations are $\overline{\boldsymbol{x}}_m(t)$, while the virtual marker locations from the simulation are denoted as $\boldsymbol{x}_m$. They depend on the current configuration of the model $\tilde{\boldsymbol{q}}$, that itself depends on the incremental update $\boldsymbol{f}(\Delta\boldsymbol{q})$.

$$
\min_{\Delta\boldsymbol{q}} \quad J = \sum_{m=1}^{24}\sum_{t=1}^{T} ||\overline{\boldsymbol{x}}_m(t) - \boldsymbol{x}_m\left(\tilde{\boldsymbol{q}}(\boldsymbol{f}(\Delta\boldsymbol{q})), \boldsymbol{\varrho}_m, t\right)||^2 \tag{2}
$$

Rating the results by the average deviation in measured and simulated trajectories shows the following. Personalizing the dimensions of the hand model without considering personalized local marker coordinates has no or only minor effects on the residual error compared to the generic model. However, additionally considering personalized local coordinates reduces the residual by $\frac{3}{4}$ compared to the generic model and the average marker deviation is around 5 mm. The constraint optimization on the other hand, does not decrease the residual error enough to increase the accuracy of the inverse kinematic simulation.

Acknowledgements
This work was supported by the Deutsche Forschungsgemeinschaft (DFG, German Research Foundation) under Grant SFB 1483–Project-ID 44241933.

References

[1] Phutane, U. et. al: *Evaluation of Optical and Radar Based Motion Capturing Technologies for Characterizing Hand Movement in Rheumatoid Arthritis - a Pilot Study.* Sensors, 2021.

[2] Buchholz, B. et al: *Anthropomorphic data for describing the kinematics of the human hand.* Ergonoics, 1992

[3] Wörnle, C: *Mehrkörpersysteme.* Springer, 2016

[4] Phutane, U. et al: *Kinematic validation of a human thumb model.* ECCOMAS - Thematic Conference on Multibody Dynamics, 2017

[5] Zhang, X. et al: *Determining finger segmental centers of rotation in flexion-extension based on surface marker measurement.* Journal of Biomechanics, 2003

A transmural path model to compute the orthotropic tissue structure in heart simulations

David Holz, Minh Tuan Duong, Denisa Martonová, Muhannad Alkassar[1], Sigrid Leyendecker

In the past decades, the structure of the heart, human as well as other species, has been explored in a detailed way, e.g., via histological studies or diffusion tensor magnetic resonance imaging. Nevertheless, the assignment of the characteristic orthotropic structure in a patient-specific finite element model remains a challenging task. Various types of rule-based models, which define the local fibre and sheet orientations depending on the transmural depth, have been developed. However, the correct assessment of the transmural depth is not trivial, see Fig. 1. Its accuracy has a substantial influence on the overall mechanical and electrical properties in rule-based models.

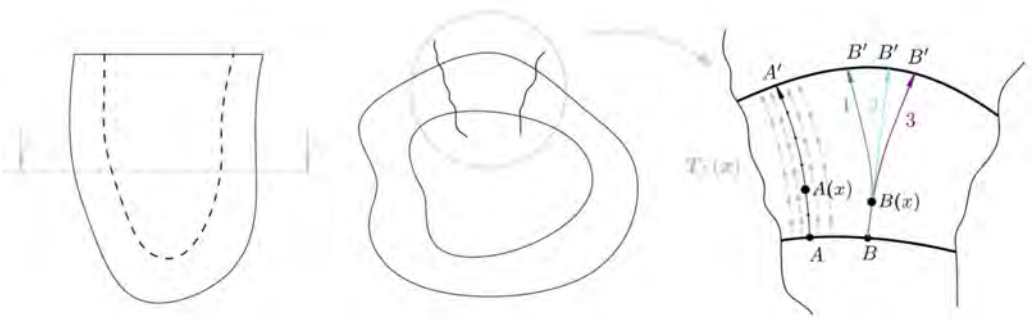

Figure 1: Representation of the transmural path in a 2D slice of the left ventricle as an example to show the complexity of the proper assessment of the transmural depth. From three arbitrary sketched paths (1–3) on the right, all seem to be a plausible transmural path through any point $B(x)$ in the domain. The path A–A' is obtained by the solution of Eq. (1) and Eq. (2). The Figure is originally published in [4].

The main purpose of this study (more details can be found in [4]) is the development of a finite element-based approach to accurately determine the transmural depth on a general unstructured grid. Instead of directly using the solution of the Laplace problem as the transmural depth, we make use of a well-established model for the assessment of the transmural thickness, see [1, 2]. It is based on two hyperbolic first-order partial differential equations for the definition of a transmural path, whereby the transmural thickness is defined as the arc length of this path.

Following the approach in [2], we compute the arc length functions of the corresponding transmural path to endocardium ($L_0(\boldsymbol{x})$, in Eq. (1) and Fig. 1 path $A(\boldsymbol{x})$–A) and epicardium ($L_1(\boldsymbol{x})$, in Eq. (2) and Fig. 1 path $A(\boldsymbol{x})$–A') starting at an arbitrary considered point $\boldsymbol{x}$ in the domain by the following hyperbolic first-order PDEs:

$$\nabla L_0(\boldsymbol{x}) \cdot \boldsymbol{T}_f(\boldsymbol{x}) = 1 \qquad \text{in } \mathcal{H} \tag{1}$$

$$-\nabla L_1(\boldsymbol{x}) \cdot \boldsymbol{T}_f(\boldsymbol{x}) = 1 \qquad \text{in } \mathcal{H} \tag{2}$$

with $L_0(\boldsymbol{x}) = 0$ for $\boldsymbol{x} \in \partial\mathcal{H}_0$ and $L_1(\boldsymbol{x}) = 0$ for $\boldsymbol{x} \in \partial\mathcal{H}_1$. We solve Eq. (1) and Eq. (2) in the framework of a finite-element based discontinuous Galerkin approach (DG), see also [3]. Based on the accurate transmural depth, we assign the local material orientation of the orthotropic tissue structure in a usual fashion. We show that this approach leads to a more accurate definition of the transmural depth, see Fig. 2 right. Furthermore, for the left ventricle, we propose functions for the transmural fibre and sheet orientations by fitting them to the literature-based diffusion tensor magnetic resonance imaging data. For more details see [4]. The proposed functions provide a distinct improvement compared to existing rules from the literature.

In the work in [4], we propose a discontinuous Galerkin-based approach in order to accurately assess the transmural thickness and depth on the same unstructured finite-element mesh like the subsequent heart simulation. We show that the accurate transmural depth results in an improved definition of the orthotropic tissue structure

[1]Pediatric Cardiology, Friedrich-Alexander-Universität Erlangen-Nürnberg, Loschgestrasse 15, 91054 Erlangen, Germany

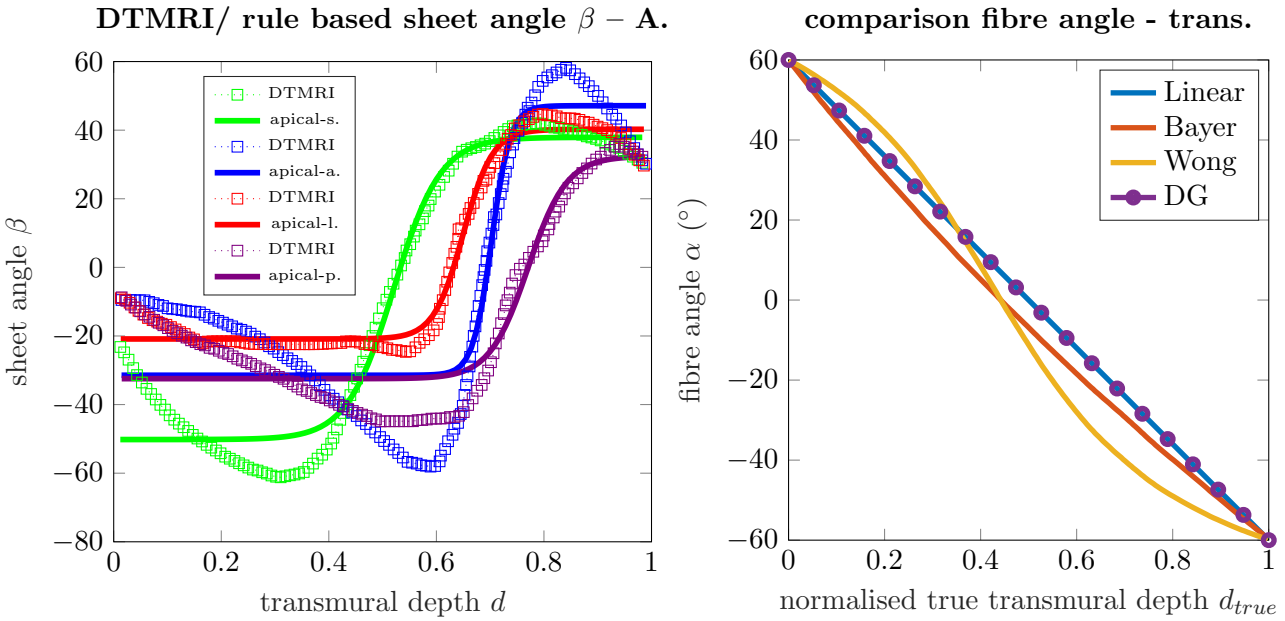

Figure 2: On the left, the fitted functions for the sheet angle β is shown for the the defined regions of the myocardium. On the right, the plot shows the different results based on a linear rule for the fibre angle α over the normalised true transmural depth d_{true}. The desired linear change (blue) in fibre angle can be achieved by utilisation of the proposed DG approach. The Fig. is originally published in [4].

in finite element models. The approach is straightforward to implement, efficient and accurate. The method can be used for more complex domains, e.g., biventricular or atrial structures. Additionally, this approach can readily be applied to assess the thickness of any finite-element domain. The proposed functions for the fibre angle α and sheet angle β show a distinct improvement compared to existing rules in order to fit DTMRI derived functions.

Acknowledgment This work is funded by the Klaus Tschira Stiftung grant 00.289.2016

References

[1] S. E. Jones, B. R. Buchbinder, I. Aharon. *Three–dimensional mapping of cortical thickness using Laplace's equation.* Human brain mapping **11:1**, 12–32 (2000).

[2] A. J. Yezzi, J. L. Prince. *An Eulerian PDE approach for computing tissue thickness* IEEE **22:10**, 1332–1339 (2003).

[3] F. Brezzi, L. D. Marini, E. Süli. *Discontinuous Galerkin methods for first-order hyperbolic problems* Mathematical models and methods in applied sciences **14:12**, 1893–1903 (2004).

[4] D. Holz, M. T. Dong, D. Martonová, M. Alkassar, S. Leyendecker. *A Transmural Path Model Improves the Definition of the Orthotropic Tissue Structure in Heart Simulations* Journal of Biomechanical Engineering – American Society of Mechanical Engineers **144:2**, 031002 (2021).

Electromechanically coupled beam models for stacked dielectric elastomer actuators

Dengpeng Huang, Sigrid Leyendecker

In this project, we are interested in numerical modelling of the soft robotics actuated by the Dielectric Elastomer Actuators (DEAs). In DEA, the silicon polymer is sandwiched between two compliant electrodes, as shown in Fig. 1. By applying the external electrical field, the polymer chains will be polarized leading to the attractive forces and deformations in the DEA.

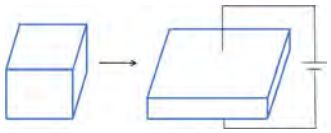

Figure 1: Working principle of DEA.

The beam model of the DEA has been developed in [1], where the kinematics, the constitutive law and the governing equations are formulated as following

Mechanical kinematics

$$\mathbf{x}(X^k, s, t) = \boldsymbol{\varphi}(s, t) + X^k \mathbf{d}_k(s, t)$$
$$\mathbf{F}(X^k, s) = \frac{\partial \mathbf{x}}{\partial X_i} \otimes \mathbf{d}_i(s, 0) = \left[\mathbf{I} + \left(\boldsymbol{\gamma} + \boldsymbol{\kappa} \times X^k \mathbf{d}_k\right) \otimes \mathbf{d}_3\right] \boldsymbol{\Lambda}$$

Electrical kinematics

$$\phi(X^k, s) = \phi_o(s) + X^1 \alpha(s) + X^2 \beta(s)$$
$$\mathbf{E}^e(X^k, s) = -\frac{\partial \phi}{\partial X_i} \mathbf{d}_i^0 = - \left[\alpha \mathbf{d}_1^0 + \beta \mathbf{d}_2^0 + (\frac{\partial \phi_o}{\partial s} + X^1 \frac{\partial \alpha}{\partial s} + X^2 \frac{\partial \beta}{\partial s}) \mathbf{d}_3^0\right]$$

$$\Omega_b(\boldsymbol{\gamma}, \boldsymbol{\kappa}, \boldsymbol{\varepsilon}, \mathbf{e}) = \int_\Sigma \Omega(\mathbf{C}, \mathbf{E}^e) dA$$

Balance of momentum

$$\begin{aligned} \nabla_{\mathbf{X}} \cdot \mathbf{P} + \rho_0 \bar{\mathbf{b}} &= \rho_0 \ddot{\mathbf{u}} && \text{in } B \\ \mathbf{F}\mathbf{P}^T &= \mathbf{P}\mathbf{F}^T && \text{in } B \\ \mathbf{P}\mathbf{N} &= \bar{\mathbf{T}} && \text{on } \partial B_\sigma \\ \mathbf{u} &= \bar{\mathbf{u}} && \text{on } \partial B_u \end{aligned}$$

Balance of momentum in beam

$$\begin{aligned} \partial_s \mathbf{f} + \bar{\mathbf{f}} &= \rho A \ddot{\mathbf{u}} && s \in [0, L] \\ \partial_s \mathbf{m} + \partial_s \mathbf{u} \times \mathbf{f} + \bar{\mathbf{m}} &= \mathbb{I}\dot{\boldsymbol{\omega}} + \boldsymbol{\omega} \times \mathbb{I}\boldsymbol{\omega} && s \in [0, L] \\ \mathbf{f} = \bar{\mathbf{f}},\ \mathbf{m} &= \bar{\mathbf{m}} && \text{at } s_\sigma \\ \mathbf{u} &= \bar{\mathbf{u}} && \text{at } s_u \end{aligned}$$

Maxwell equation

$$\begin{aligned} \nabla_{\mathbf{X}} \times \mathbf{E}^e = \mathbf{0}, \quad \nabla_{\mathbf{X}} \cdot \mathbf{D} &= 0 && \text{in } B \\ \mathbf{D} \cdot \mathbf{N} &= \bar{Q} && \text{on } \partial B_q \\ \phi &= \bar{\phi} && \text{on } \partial B_\phi \end{aligned}$$

Maxwell equation in beam

$$\begin{aligned} \partial_s d_{1s}^e + \bar{q} &= 0 && s \in [0, L] \\ q &= \bar{q} && \text{at } s_q \\ \phi &= \bar{\phi} && \text{at } s_\phi \end{aligned}$$

Constitutive law

$$\mathbf{P} = \frac{\partial \Omega(\mathbf{F}, \mathbf{E}^e)}{\partial \mathbf{F}}$$
$$\mathbf{D} = -\frac{\partial \Omega(\mathbf{F}, \mathbf{E}^e)}{\partial \mathbf{E}^e}$$

Constitutive law in beam

$$\mathbf{f} = \frac{\partial \Omega_b(\boldsymbol{\gamma}, \boldsymbol{\kappa}, \boldsymbol{\varepsilon}, \mathbf{e})}{\partial \boldsymbol{\gamma}}, \mathbf{m} = \frac{\partial \Omega_b(\boldsymbol{\gamma}, \boldsymbol{\kappa}, \boldsymbol{\varepsilon}, \mathbf{e})}{\partial \boldsymbol{\kappa}}$$
$$\mathbf{d}_1^e = \frac{\partial \Omega_b(\boldsymbol{\gamma}, \boldsymbol{\kappa}, \boldsymbol{\varepsilon}, \mathbf{e})}{\partial \boldsymbol{\varepsilon}}, \mathbf{d}_2^e = \frac{\partial \Omega_b(\boldsymbol{\gamma}, \boldsymbol{\kappa}, \boldsymbol{\varepsilon}, \mathbf{e})}{\partial \mathbf{e}}$$

with ϕ the electric potential, $\mathbf{F}$ the deformation gradient, $\mathbf{E}^e$ the electrical field, Ω the strain energy, Ω_b the strain energy of beam, $\boldsymbol{\varepsilon}$ and $\mathbf{e}$ the strain-like electrical variables conjugated with the electric displacements $\mathbf{d}_1^e$ and $\mathbf{d}_2^e$, $\boldsymbol{\gamma}$ and $\boldsymbol{\kappa}$ the beam strain measures, $\mathbf{D}$ the electric displacement, $\mathbf{P}$ the first Piola-Kirchhoff stress tensor, $\mathbf{f}$ the internal force, $\bar{\mathbf{f}}$ the external force, $\mathbf{m}$ the torque per unit of arch-length, $\boldsymbol{\omega}$ the spatial angular velocity, $\mathbb{I}$ the spatial mass moment of inertia tensor, ρ_0 the mass density in initial configuration, $\bar{\mathbf{b}}$ the body force vector. The details on beam mechanical kinematics can be found in [2].

By applying proper electric potential on the bean cross sections, the deformations such as contraction, bending, shear and torsion can be actuated in the beam. As an example of the combination of different deformation modes, the beam model is applied in [1] to simulate a simplified robotic arm holding a package as shown in Fig. 2. The package is represented by an additional point mass concentrated at the beam's free end. The mass of package is set to be 2 times the mass of beam.

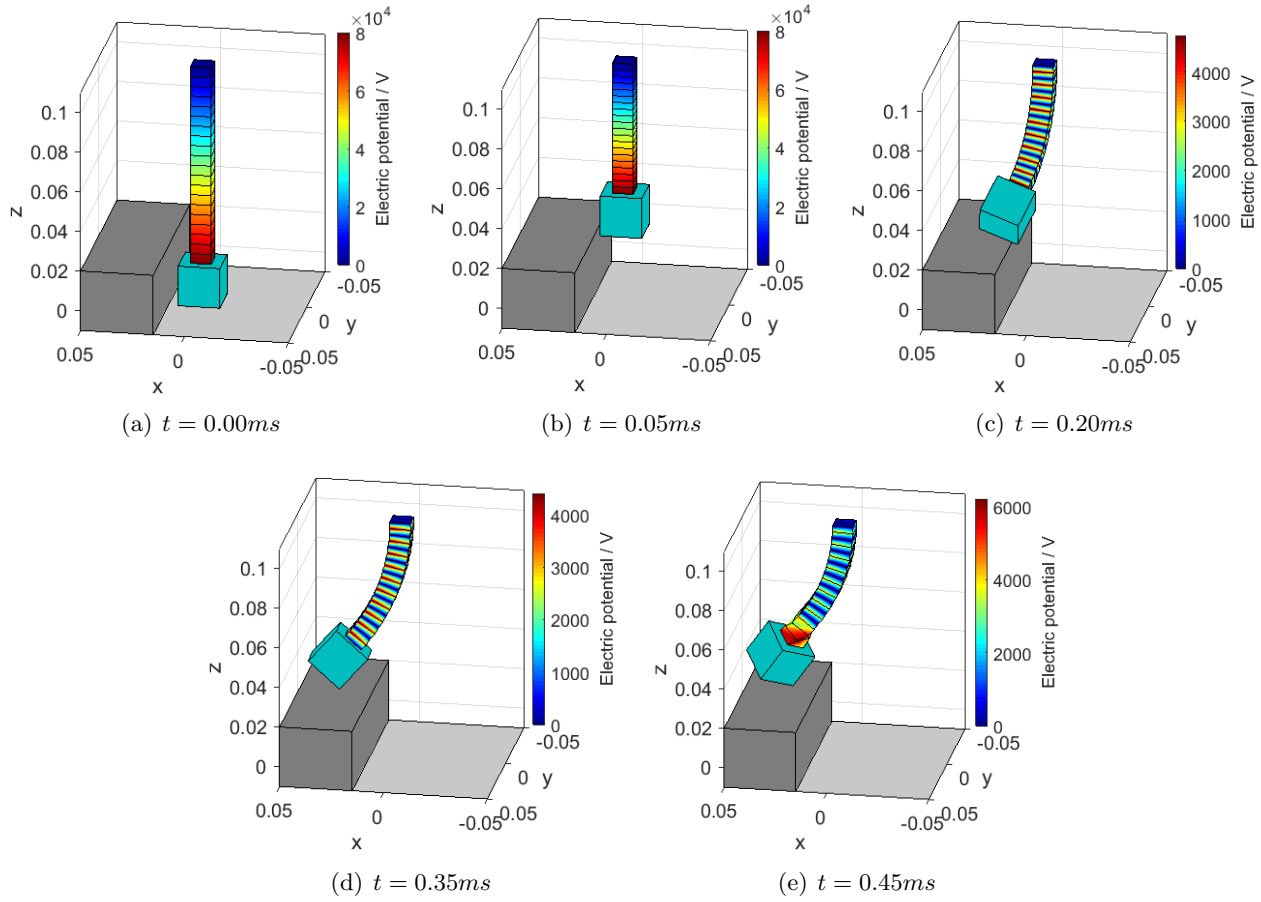

(a) $t = 0.00ms$ (b) $t = 0.05ms$ (c) $t = 0.20ms$

(d) $t = 0.35ms$ (e) $t = 0.45ms$

Figure 2: A soft robotic arm moving a package from the ground to a desk.

References

[1] D. Huang, S. Leyendecker. An electromechanically coupled beam model for dielectric elastomer actuators. Computational Mechanics, 2021. DOI:10.1007/s00466-021-02115-0.

[2] F. Auricchio, P. Carotenuto, and A. Reali. On the geometrically exact beam model: a consistent, effctive and simple derivation from three-dimensional finite-elasticity. International Journal of Solids and Structures, 45(17):4766-4781, 2008.

Smoothed finite element method in modelling and simulation of active cardiac mechanics

Denisa Martonová, David Holz, Minh Tuan Duong, Sigrid Leyendecker

In the last decades, various computational models have been developed to simulate cardiac electromechanics. The most common numerical tool is the finite element method (FEM). However, it is known that this method crucially depends on the mesh quality. For complex geometries such as cardiac structures, it is convenient to use tetrahedral discretisations which can be generated automatically. On the other hand, such automatic meshing with tetrahedrons in combination with large deformations often lead to elements distortion and volumetric locking. To overcome these difficulties, different smoothed finite element methods (S-FEMs) have been proposed in the recent years [4, 5]. S-FEMs are known to be volumetric locking free, less sensitive to mesh distortion and so far have been used e.g. in simulation of passive cardiac mechanics [2]. In our recent work [5], we extend for the first time node-based S-FEM (NS-FEM), firstly proposed in [3], towards active cardiac mechanics.

In all S-FEMs, firstly, the domain Ω bounded by Γ is discretised into non-overlapping elements in the same way as in the FEM. Subsequently, it is subdivided into a finite number of non-overlapping smoothing domains (SDs) Ω_k with boundary Γ_k, i.e. $\Omega = \cup_{k \in n_{sd}} \Omega_k$, where n_{sd} is the number of SDs and $\Omega_i \cap \Omega_j = \emptyset$ for $i \neq j$. We refer to Figure 1 for SDs in 2D for NS-FEM. The key idea of S-FEMs is gradient smoothing over a SD Ω_k by convolution with a smoothing function Φ_k satisfying at least the property $\int_{\Omega_k} \Phi_k(\boldsymbol{X}) \mathrm{d}\Omega = 1$, e.g.

$$\Phi_k(\boldsymbol{X}) = \begin{cases} 1/V_k & \text{if } \boldsymbol{X} \in \Omega_k \\ 0 & \text{else} \end{cases} \quad \text{with } V_k = \int_{\Omega_k} \mathrm{d}\Omega. \tag{1}$$

Assuming a geometrically non-linear 2D problem and linear triangular elements, the smoothed deformation gradient $\bar{\boldsymbol{F}}^k$ is constant for all material points $\boldsymbol{X}_k \in \Omega_k$ and takes the form

$$\bar{F}^k_{iJ}(\boldsymbol{X}_k) = \int_{\Omega_k} F^e_{iJ}(\boldsymbol{X}) \Phi_k(\boldsymbol{X}) \mathrm{d}\Omega = \frac{1}{V_k} \sum_{e \in n^e_k} \frac{V_e}{3} \frac{\partial u^e_i(\boldsymbol{X})}{\partial X_J} + \delta_{iJ} \tag{2}$$

where V_e is the area of the element e and n^e_k is the set of elements connected to the node k in NS-FEM.

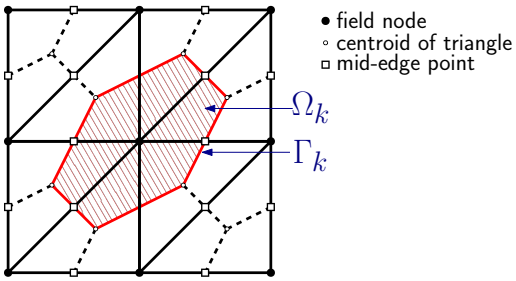

Figure 1: Smoothing domains in 2D for NS-FEM. The Figure is originally published in [5].

In our recent work [5], an active contraction in circumferentially aligned fibre orientation according to [1] is modelled in the healthy and the infarcted case as depicted in Figures 2 and 3, respectively. Here, the active fibre tension depends on the time and the current deformation. The maximal fibre tension T_{max} is set to 5 kPa and 0 kPa in the healthy and infarcted regions, respectively. In [5], we show that the proposed method is more robust with respect to mesh distortion and computationally more efficient than standard FEM. Being furthermore free of volumetric locking problems makes S-FEM a promising alternative in modelling of active cardiac mechanics, respectively electromechanics[5].

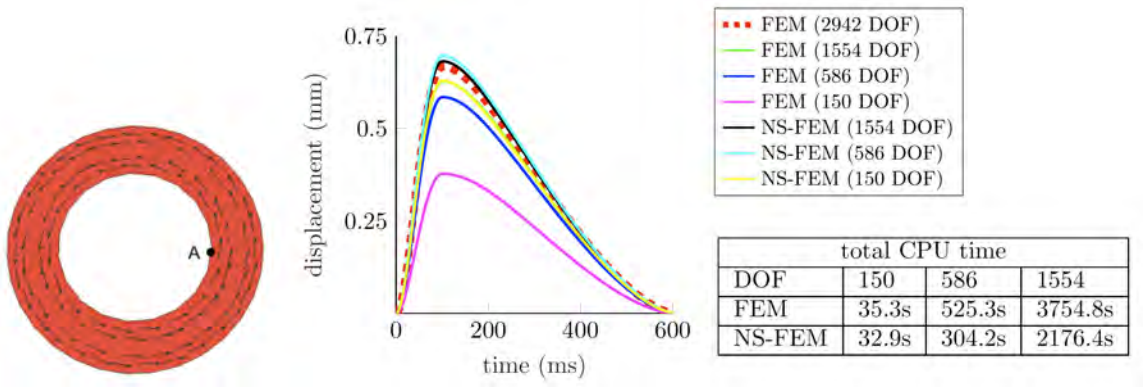

total CPU time			
DOF	150	586	1554
FEM	35.3s	525.3s	3754.8s
NS-FEM	32.9s	304.2s	2176.4s

Figure 2: Left to right: undeformed healthy ventricular slice with the circumferentially aligned fibre orientation; displacement of the node A with $T_{max} = 5$ kPa; total CPU time for simulations using FEM and NS-FEM with different DOFs. The Figure is originally published in [5].

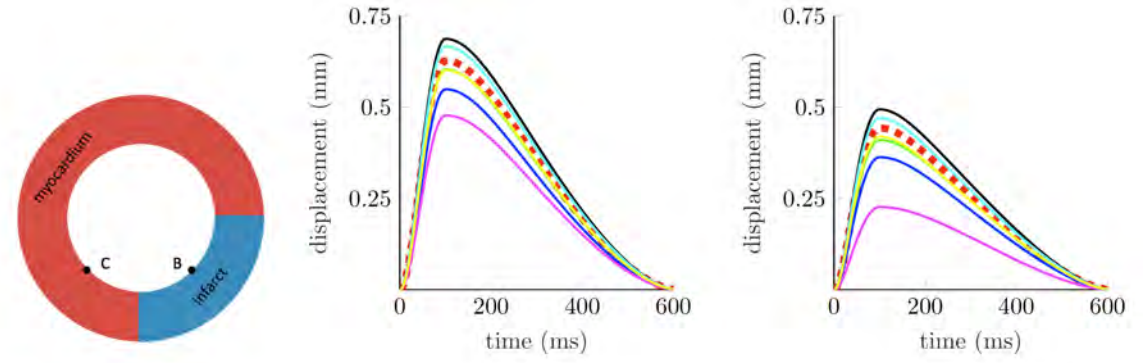

Figure 3: Left to right: schematic representation of the ventricular slice with myocardial infarction in the fourth quadrant; displacement of the node C in the healthy region ($T_{max} = 5$ kPa); displacement of the node B in the infarcted region ($T_{max} = 0$ kPa). The Figure is originally published in [5].

Acknowledgments This work is funded by the Klaus Tschira Stiftung grant 00.289.2016.

References

[1] J. M. Guccione, L. K.Waldman, A. D. McCulloch. *Mechanics of Active Contraction in Cardiac Muscle: Part II— Cylindrical Models of the Systolic 219 Left Ventricle.* J. Biomech. Eng. 115 (1993).

[2] C. Jiang, G.R. Liu, X. Han, Z.Q. Zhang, W. Zeng *A Smoothed Finite Element Method for Analysis of Anisotropic Large Deformation of Passive Rabbit Ventricles in Diastole.* Int. J. Numer. Method. 31(2015).

[3] G. R. Liu, T. Nguyen-Thoi, H. Nguyen-Xuan, K. Y. Lam. *A Node-Based Smoothed Finite Element Method (NS-FEM) for Upper Bound Solutions to Solid Mechanics Problems.* Comput. Struct. 87 (2009).

[4] G. R. Liu. *The Smoothed Finite Element Method (S-FEM): A Framework for the Design of Numerical Models for Desired Solutions.* Front. Struct. Civ. 13 (2019).

[5] D. Martonová, D. Holz, M. T. Duong, S. Leyendecker. *Towards the Simulation of Active Cardiac Mechanics Using a Smoothed Finite Element Method.* J. Biomech. 115 (2021).

CyberGlove for Clinical Use

Johannes Michaelis[2], Isabella Reiher[2], Simon Heinrich, Birte Coppers[1], Anna-Maria Liphardt[1], Sigrid Leyendecker

The CyberGlove was initially developed by CyberGloveSystems LLC for capturing hand movements in the movie industry and to prototype and animate in virtual reality [1]. However, the analysis of hand movements can yield useful information and indicators for the detection of diseases at an early stage such as rheumatic arthritis. There is currently a lack of measurement systems for hand motion that can be used easily in a clinical setting. The goal of this work is to analyze whether the glove bears potential for this purpose. This is done by analyzing the accuracy of a calibration process followed by measurements during daily living.

Figure 1: Close-up of the CyberGlove.

Figure 2: CyberGlove with arm pouch.

The Cyberglove — shown in Fig. 1 — has twenty-two sensors sewed in at each joint to measure movement. These sensors are thin wires with an electrical resistance that changes proportionally to their elongation. The sensors provide byte values, that are transmitted via TCP by a microcontroller on the upper arm, as in Fig. 2. The glove is only suitable for a certain range of hand sizes, as it is only available in one size. Therefore, hand size limits have to be found. A complex calibration process is required to calculate reliable angles. This calibration has to be done by every subject, since the fit differs between subjects [2].

Figure 3: Simple calibration procedure with different static postures and predefined angles.

A linear relationship is assumed between the output of each sensor and the corresponding joint angle. Thus, two measurements per sensor are sufficient, see Fig. 3. This approach meets expectations for simple flexion angles but shows implausible results if flexion and abduction is combined. For the calculation of abduction angles, adjacent sensors must also be considered due to cross-coupling effects. Several publications as [2, 3] propose different approaches based on capturing movements over time instead of static postures. Root-mean-square error minimization is performed to obtain the gains and fitting factors of various given polynomials. A similar approach is used for the thumb. With this all gains to calculate from measured values to useful joint angles can be determined by the calibration, with exception for the angles at the thumb carpometacarpal joint.

[1]Department of Internal Medicine 3 - Rheumatology and Immunology, University Hospital Erlangen, FAU, Erlangen, Germany

[2]These authors contributed equally to this work.

To get the missing parameters for the thumb, a closed-loop motion is captured — as in Fig. 4 — in which the thumb and index finger remain in tip contact during extension and flexion. Then the gains of the thumb carpometacarpal joint are determined by minimizing the distance between the fingertips using a kinematic hand model.

Figure 4: Closed-loop motion kinematic hand model.

In general, measuring motion instead of static poses can compensate for measurement errors and is therefore less influenced by an incorrect hand posture or a disturbed measurement signal. It has the potential to be more accurate and reliable than the calibration with static poses. It is to be investigated whether measuring more than two static poses per flexion angle with a linear relationship can also improve the results.
Since the calibration process for a clinical application needs to be performed on both healthy subjects and impaired patients, the procedure must also be applicable to patients with hand movement limitations. To achieve such applicability, either the hand postures may need to be adjusted or a cross-subject calibration may need to be applied. The latter may reduce the accuracy of the angle calculation, but would be faster since the subject only needs to set a neutral hand posture as all gains are already calculated. Whether the use of a cross-subject calibration would be helpful in conducting a study with arthritis patients remains to be determined.

References

[1] CyberGloveSystemsLLC *CyberGlove III Datasheet* (2010)

[2] Eccarius, Petra; Bour, Rebecca; Scheidt, Robert A. *Dataglove measurement of joint angles in sign language handshapes* (2012)

[3] Gracia-Ibáñez, Verónica; Vergara, Margarita; Buffi, James H.; Murray, Wendy M.; Sancho-Bru, Joaquín L. *Across-subject calibration of an instrumented glove to measure hand movement for clinical purposes* (2017)

Dynamic phase-field model for the brittle fracture

Dhananjay Phansalkar, Michael Ortiz[1], Kerstin Weinberg[2], Sigrid Leyendecker

The fracture mechanics describe the state mechanical system during crack initiation, nucleation, and propagation. Typically, based on material behaviour, the modeling of fracture can be distinguished into brittle and ductile fractures. We observe brittle fracture in materials such as glass, ceramics, cast iron and graphite, etc., ductile fracture in aluminium, steel, copper, etc. These fractures can be modeled as a discrete crack (leading to numerical difficulties) or a diffused crack ()resulting in a decrease in accuracy)[1]. However, in this project, we are interested in simulating diffused cracks with improved accuracy and lowered computational cost. The approach we took in a quasi-static regime to progress along this direction can be explored in our submitted paper [2]. Nonetheless, when we observe complex cracks in our daily lives, these crack paths occur in a dynamic setting in which inertial effects and rate-dependent rapid loading must be taken into account.

We investigate these dynamic effects in crack propagation under the framework of the phase-field model. The action for such a system is given by the standard dynamic phase-field model [3]

$$\begin{aligned} E(\boldsymbol{u}, \dot{\boldsymbol{u}}, c) &= \int_0^T \int_\Omega \left[\frac{1}{2}\rho \dot{\boldsymbol{u}} \cdot \dot{\boldsymbol{u}} - [1-c]^2 \psi(\boldsymbol{\varepsilon}) - \mathcal{G}_c \left[\frac{c^2}{2\epsilon} + \frac{\epsilon}{2} |\nabla c|^2 \right] \right] d\boldsymbol{x}\ dt \\ \psi(\boldsymbol{\varepsilon}) &= \frac{1}{2}\boldsymbol{\varepsilon}(\boldsymbol{u}) : [\mathbb{C}\boldsymbol{\varepsilon}(\boldsymbol{u})] = \frac{1}{2}\lambda[\mathrm{tr}(\boldsymbol{\varepsilon})]^2 + \mu[\boldsymbol{\varepsilon} : \boldsymbol{\varepsilon}] \end{aligned} \tag{1}$$

where T, $\boldsymbol{u}$, $\dot{\boldsymbol{u}}$, c, and $\boldsymbol{\varepsilon}$ are the end time, displacement field, velocity field, phase field and strain tensor respectively. ϵ is a constant regularisation parameter, and ρ, $\mathcal{G}_c$, λ and μ are material parameters. Stationary point of the action (1) with respect to $\boldsymbol{u}$ and c yields the following Euler-Lagrange equations

$$\begin{aligned} \nabla \cdot \boldsymbol{\sigma} &= \rho \ddot{\boldsymbol{u}} \quad \text{in} \quad \Omega \times (0,T] \\ \frac{c\mathcal{G}_c}{\epsilon} - 2\,[1-c]\,\psi(\boldsymbol{\varepsilon}) - \mathcal{G}_c \nabla \cdot [\epsilon \nabla c] &= 0 \quad \text{in} \quad \Omega \times (0,T]. \end{aligned} \tag{2}$$

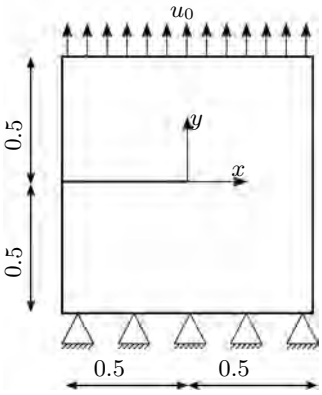

Figure 1: 2D problem set-up

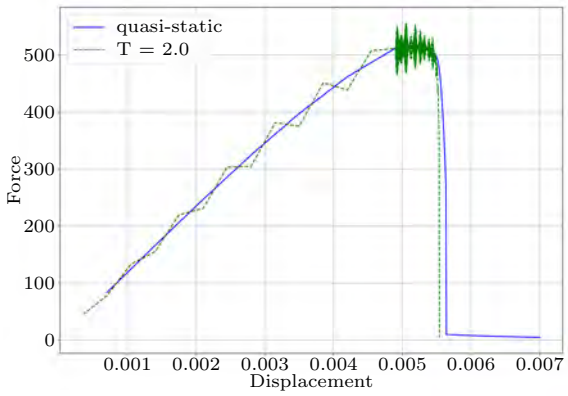

Figure 2: Force vs displacement plot

In addition to these equations of motion (2), the typical initial and boundary conditions for phase-field problems are $\boldsymbol{u}(\boldsymbol{x},0) = \boldsymbol{g}_0(\boldsymbol{x}) = 0$ and $\boldsymbol{x} \in \overline{\Omega}$, $\dot{\boldsymbol{u}}(\boldsymbol{x},0) = \boldsymbol{v}_0(\boldsymbol{x}) = 0$ and $\boldsymbol{x} \in \overline{\Omega}$ and $\boldsymbol{u} = \boldsymbol{u}_0$ on $\partial\Omega_\mathrm{d} \times (0,T]$, $\boldsymbol{c} = \boldsymbol{c}_0$ on $\partial\Omega_\mathrm{p} \times (0,T]$, $\nabla c \cdot \boldsymbol{n} = 0$ on $\partial\Omega \setminus \partial\Omega_\mathrm{p} \times (0,T]$ respectively. The domain is discretized with finite elements and the problem is solved using a staggered approach for robustness. Furthermore, we validated the dynamic phase-field implementation comparing the force vs. displacement curve between the dynamic and the quasi-static scenario Figure 2 for a Single Edge Notch Tension (SENT) specimen as seen in Figure 1.

[1]Division of Engineering and Applied Sciences, California Institute of Technology, California, USA
[2]Lehrstuhl für Festkörpermechanik, Universität Siegen, 57076 Siegen, Germany

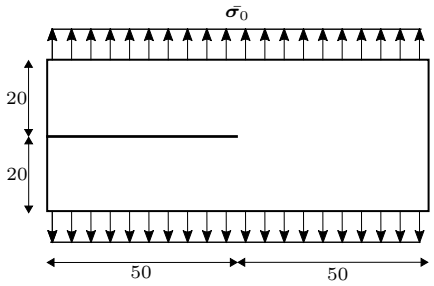

Figure 3: 2D problem for crack branching

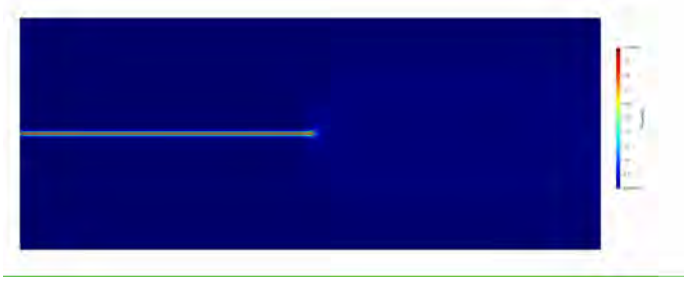

Figure 4: Initial crack with phase field

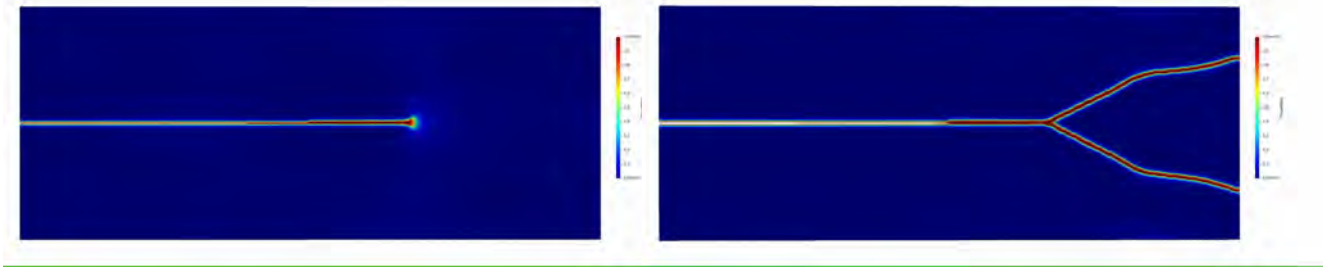

Figure 5: Evolution of phase field showing crack branch

With the valid implementation, we simulated a problem with traction on the boundary Figure 3. The initial phase field can be seen in Figure 4, and the evolution of the phase-field, showing crack branching, is depicted in Figure 5. The future steps in our project is to extend our model, the spatially adaptive phase-field model in the dynamic case.

Acknowledgement : The German Research Foundation (DFG) is gratefully acknowledged for funding this research within the research training group GRK2423 FRASCAL.

References

[1] A. Egger, U. Pillai, K. Agathos, E. Kakouris, E. Chatzi, I.A. Aschroft and S.P Triantafyllou. *Discrete and Phase Field Methods for Linear Elastic Fracture Mechanics: A Comparative Study and State-of-the-Art Review*. Applied Sciences, 9:2436, 2019.

[2] D. Phansalkar, K. Weinberg, M. Ortiz, Michael and S. Leyendecker. *A Spatially Adaptive Phase-Field Model of Fracture*, arXiv:2109.10175 [cs, math], 2021.

[3] M.J. Borden,C.V. Verhoosel, M.A. Scott, T.J.R. Hughes and C.M. Landis. *A Phase-Field Description of Dynamic Brittle Fracture*. Computer Methods in Applied Mechanics and Engineering, 217-220:77-95, 2012.

[4] H. Amor, J-J. Marigo and C. Maurini. *Regularized Formulation of the Variational Brittle Fracture with Unilateral Contact: Numerical Experiments*. Journal of the Mechanics and Physics of Solids, 57:1209-1229, 2009.

Several topics on variational integrators

Rodrigo T. Sato Martín de Almagro, Sigrid Leyendecker

Geometric integration involves the numerical solution of differential equations using methods that intend to preserve some or all features or underlying structures that the original problem displays.

One particular set of geometric integration methods that our chair is interested in is variational methods [1, 2]. These are numerical methods tailored to systems whose behaviour can be derived from a variational principle, e.g. Hamilton's principle of stationary action, and related systems. These systems display important qualitative features that should ideally be present in the results of a simulation, such as conservation laws due to symmetries in the system (Noether's theorem) or compliance with specified constraints.

Variational methods are already being applied every day in the study and simulation of standard mechanical systems such as systems of particles and rigid bodies, as well as optimal control problems, where the dynamics are governed by ordinary differential equations. But these can also be applied to field theories, where the resulting equations are partial differential equations. These include the equations of finite strain elasticity, perfect fluids, electrodynamics... The study and use of variational methods on fields is still not as extended or well-understood as in the former. For that matter, we are trying to understand the basics of these methods.

We are currently focusing on the following topics:

- **Parallelized variational integrators.** Solving boundary value problems in the context of optimal control of particle systems can be a costly endeavour, particularly for real-time applications. We have analysed the convergence properties of parallelized versions of variational integrators for their implementation in graphics processing units, a.k.a GPUs [4]. In figure 1: How do you steer a constant-thrust ship to navigate between given points through wind in the minimum time? Different locally optimal solutions of the Zermelo navigation problem solved with a parallel method.

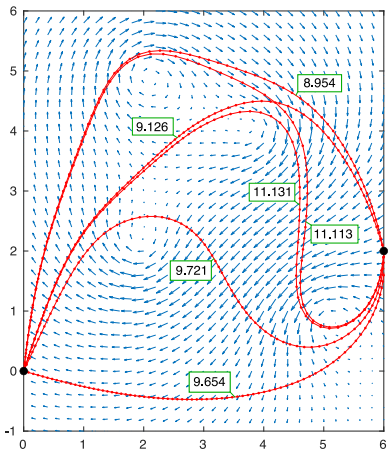

Figure 1

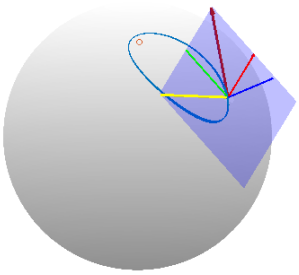

Figure 2

- **Methods on homogeneous spaces.** Homogeneous spaces are frequently said to be spaces where every point looks exactly the same as every other point, e.g. the sphere. We have successfully extended previous work on nonholonomic integrators on Lie groups [7, 8] to this setting [5]. These methods, although not completely variational, extend these naturally in this context, displaying similar behaviour. In figure 2: The Kepler problem on a sphere. The red circle plays the role of a star and the blue line represents the orbit of a planet in this small spherical universe.

- **Behaviour of multisymplectic methods.** We are studying multi-symplectic methods [3, 6] in the framework of variational integrators to better understand the properties and expected behaviour of these methods as well as obtain insight into the generation of more general methods. Our main goal is to perform structure-preserving integration of the geometrically exact beam (GEB) (fig. 3).

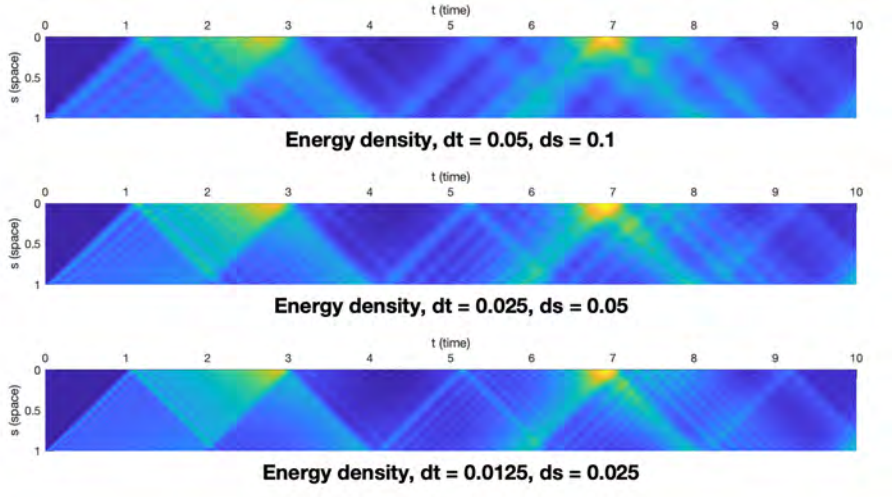

Figure 3: Energy behaviour of the GEB. Evolution in time and space of the energy density of a cantilevered beam under an axial and tangential point loads at the free end. Results on three different grids are displayed.

References

[1] J. E. Marsden and M. West. Discrete mechanics and variational integrators. *Acta Numerica*, 10:357-514, 2001.

[2] E. Hairer, C. Lubich, and G. Wanner. Geometric numerical integration: structure preserving algorithms for ordinary diferential equations. *Springer series in computational mathematics*. Springer, Berlin, Heidelberg, New York, 2006.

[3] T. J. Bridges and S. Reich. Multi-symplectic integrators: numerical schemes for Hamiltonian PDEs that conserve symplecticity. *Phys. Lett. A*, 284(4-5):184-193, 2001.

[4] S. J. Ferraro, D. Martín de Diego and R. T. Sato Martín de Almagro. Parallel iterative methods for variational integration applied to navigation problems. *(preprint, arXiv:2109.055 59)*. Accepted.

[5] R. T. Sato Martín de Almagro. High-order integrators on homogeneous spaces via nonholonomic mechanics. In preparation.

[6] T. Leitz, R. T. Sato Martín de Almagro, and S. Leyendecker. Multisymplectic Galerkin Lie group variational integrators for geometrically exact beam dynamics based on unit dual quaternion interpolation. *Comput. Methods Appl. Mech. Eng.*, 374:113475, 2021.

[7] R. T. Sato Martín de Almagro. Convergence of Lobatto-type Runge-Kutta methods for partitioned differential-algebraic systems of index 2. *BIT Numer. Math.*, 1572-9125, 2021

[8] D. Martín de Diego and R. T. Sato Martín de Almagro. High-order geometric methods for nonholonomic mechanical systems. *(preprint, arXiv:1810.109 26)*. Submitted.

Fuzzy forward dynamics simulation of a human leg with a prosthetic foot

Eduard S. Scheiterer, Sigrid Leyendecker

When designing complex systems, such as a prosthetic foot, simulations are used to predict and validate the design before production. These simulations require various assumptions about parameters and conditions, which usually have to be precisely and deterministicly defined. However, when measuring these parameters, absolute accuracy and therefore knowledge of the parameters is not possible. Ideally, the simulation would account for this uncertainty, which can be subdivided, based on its characteristics, into aleatoric and epistemic uncertainty. Aleatoric uncertainty or stochastic uncertainty is characterised by randomness. In contrast, epistemic uncertainty is characterised by incompleteness. Within the project SPP 1886, we are examining the propagation of polymorphic uncertainty through a model of the human leg with a prosthetic foot during normal gait. Polymorphic uncertainty means both types of uncertainty are present in the model and or data of the simulation.

The multibody model of the human leg consists of the rigid thigh and shank and a flexible prosthetic foot. The prosthesis is modelled after the Össur Vari-Flex®. This results in a multibody model with both rigid and flexible bodies, which is highly non-linear and complex. The joints are modelled with constraints, allowing for the relative movement between the bodies during gait. The resulting system is solved with a variational structure preserving integrator [1], for given initial configurations and parameters.

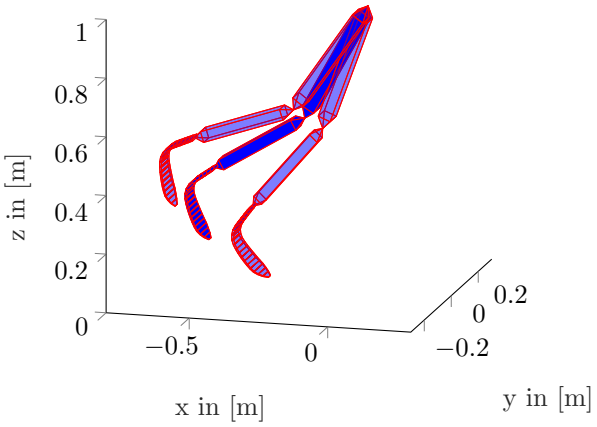

Figure 1: The initial configuration of the model (in the middle) is varied slightly (left and right, slightly transparent). The configuration is varied by changing the initial flexion angles of the hip and knee joints, in both directions.

Here, as an example, we demonstrate the effects of fuzzy initial joint angles during a swing phase simulation. The uncertainty of the initial joint angles affects the initial configuration of the leg. This means we assume incomplete information about the initial flexion angles at the hip and knee, which leads to an uncertain initial configuration and then propagate this uncertainty through the model via α-level optimisation. To do this efficiently, the Graph follower algorithm from [2] is used. As a target output quantity of interest f_d, the total deformation energy at a given time is used. This quantity is related to the comfort of the patient with a prosthetic foot during gait.

$$f_d = \sum_{el=1}^{n_{el}} W_{int,el}\left(\boldsymbol{\Gamma}(\boldsymbol{q}(\tilde{\boldsymbol{p}}, t_n), \tilde{\boldsymbol{p}}, t_n), \boldsymbol{K}(\boldsymbol{q}(\tilde{\boldsymbol{p}}, t_n), \tilde{\boldsymbol{p}}, t_n)\right) \tag{1}$$

The strain measures in the flexible prosthesis $\boldsymbol{\Gamma}(\boldsymbol{q}(\tilde{\boldsymbol{p}}, t_n), \tilde{\boldsymbol{p}}, t_n)$ and $\boldsymbol{K}(\boldsymbol{q}(\tilde{\boldsymbol{p}}, t_n), \tilde{\boldsymbol{p}}, t_n)$, based on the predeformed geometrically exact beam theory from [3], are calculated from the time node t_n, the fuzzy parameter $\tilde{\boldsymbol{p}}$ and the configuration $\boldsymbol{q}$, which also depends on the time node and fuzzy parameter. The fuzzy parameter in this case, is the initial configuration $\boldsymbol{q}_0$ at the time node $t_n = 0$.

The fuzzy uncertainty in this work is modelled as a triangular fuzzy number. This consists of an interval with a membership function, where the extreme values of the interval have the membership value $\mu_{\tilde{\boldsymbol{p}}} = 0$ and only one value within the interval has $\mu_{\tilde{\boldsymbol{p}}} = 1$. The values in between and their membership function are linearly correlated, resulting in the triangular shape.
This means the initial configuration of the leg has an interval between two extremes, visualised in Figure 1. The middle configuration is the one used for deterministic simulations, while the left and right ones, slightly transparent, are the most extreme initial positions considered here. The leg's initial configuration can be anywhere between the two cases, as long as it satisfies the joint constraints and rigid body constraints. To

propagate the fuzzy uncertainty forward through the simulation, the interval is discretised into α-level cuts. Each α-level of the input parameter also infers a membership function value for the target output, which is calculated by the α-level optimisation. This uses an optimisation to find the extreme target output values, both upper and lower, within the given input parameter interval, resulting in the upper and lower envelope for each *alpha*-level. If multiple α-levels are calculated, the results approximate the fuzzy number of the target output, based on the fuzzy input.
The simulation here emulates the swing phase during gait. The leg moves due to the gravitational field in the simulation. All other parameters of the simulation are deterministic and only the initial configuration is affected with epistemic uncertainty. Figure 2 shows the resulting envelopes for a simulation.

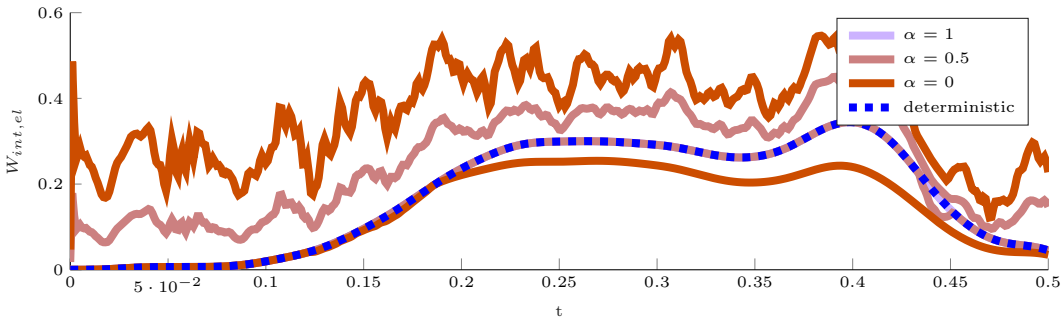

Figure 2: Envelopes of the total internal deformation energy of the prosthesis after propagating the epistemic uncertainty of the initial configuration forward through the model.

Having accomplished a fuzzy forward dynamics simulation, further work will focus on detailed modelling of uncertain parameters during gait, based on data gathered from motion capture data and interpreting the resulting envelopes to derive design recommendations. Another goal is to include polymorphic uncertainty in the simulation, expanding its capability to model realistic problems.

Acknowledgements
This work is partly supported by the German Research Foundation (DFG) as part of the Priority Programme SPP 1886 'Polymorphic uncertainty modelling for the numerical design of structures' (Grant No. LE 1841/4-2).

References

[1] Leyendecker, S.; Marsden, J.E.; Ortiz, M.: *Variational integrators for constrained dynamical systems.* ZAMM-Journal of Applied Mathematics and Mechanics, Vol. 88, p. 677-708, 2008.

[2] Eisentraudt, M. and Leyendecker, S.: *Fuzzy uncertainty in forward dynamics simulation.* Mechanical Systems and Signal Processing, 2019

[3] S. S. Antman, *Nonlinear Problems of Elasticity.* Springer, 1995.

Optimal control of a geometrically exact beam

Matthias Schubert, Sigrid Leyendecker

A geometrically exact beam is a model for the behavior of deformable objects with one dimension much larger than the other two. The dynamics of the beam are described by PDEs. We have modelled a flexible pendulum with a geometrically exact beam and posed an optimal control problem.
The beam simulation considers body load due to gravity, fixed translational degrees of freedom and external forcing playing the role of controls for the rotational degrees of freedom on one end. The other end has a free boundary. As intitial conditions, the beam points downwards. The aim of the optimal control problem is the upswing of the beam to the upright position, while minimizing the control forces.
A variational integrator is applied as equality constraints in the optimal control problem. Variational integrators show excellent long term energy behavior and preserve some geometric structure of the continous system [1]. The discrete adjoint method [2] is used to calculate exact derivatives for the objective of the optimal control problem.
The geometrically exact beam model used here is based on the multisymplecitic Galerkin Lie group variational integrator [3]. The beam equations and therefore the adjoint equations use nullspace projection as well as incremental reparametrization. For the application in optimal control, the midpoint rule in space and time is used here.

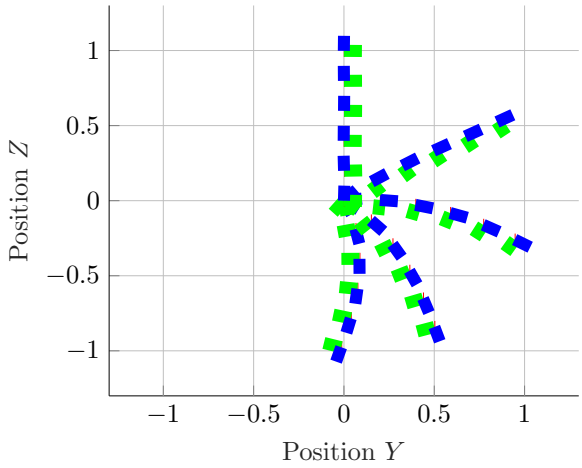

Figure 1: Snapshots of the upswing of a beam.

The optimal control problem is formulated such that the adjoint equations and the beam dynamics decouple. This allows for the sequential solution of both via forward and backward integration of the beam and the adjoint equations respectively as well as the update of the external forces in each iteration of the optimization process.

Acknowledgements This work was supported by the Deutsche Forschungsgemeinschaft (DFG, German Research Foundation) under Grant SFB 1483 Project-ID 44241933.

References

[1] Jerrold E. Marsden and Matthew West. Discrete mechanics and variational integrators. *Acta Numerica*, 10:357-514, 2001.

[2] Thomas Lauß et al. The Discrete Adjoint Gradient Computation for Optimization Problems in Multibody Dynamics. *Journal of Computational and Nonlinear Dynamics*. 031016. 2016.

[3] T. Leitz, Rodrigo T. Sato Martín de Almagro, S. Leyendecker. Multisymplectic Galerkin Lie group variational integrators for geometrically exact beam dynamics based on unit dual quaternion interpolation — no shear locking. *Computer Methods in Applied Mechanics and Engineering*. 374:113475, 2021.

Homogenized constitutive properties of multi-layered beam cross-sections

Martina Stavole, Sigrid Leyendecker

Composite materials are widely used in engineering applications. However, their constitutive properties are not easy to define due to the complex behaviour of the mixed materials. In order to analyse composite beam cross-sections, several techniques are presented in [1].

An analytical approach to determine the effective stiffness properties of composite beam cross-sections presented in [3, 2], is taken into account for the homogenization of the mechanical properties of circular multi-layered cross-sections. In [2], two-layers piecewise homogeneous sandwich beams made of isotropic materials, as shown in Fig. 1, are studied. The cross-section is divided into a core and a face, characterized by different material parameters and welded together in such a way that no separation can accur during deformation.

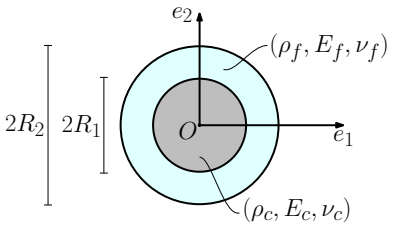

Figure 1: Circular sandwich cross-section

In [3], the mechanical behaviour of composite elastic beams is investigated by using the theory of directed curves, a Cosserat-type model for thin rods . They derive the constitutive equations for elastic composite rods in the linear theory and obtain the effective extensional, bending, shear and torsion stiffness properties of thin rods by comparing the solutions of some extension, bending and torsion problems for the directed curves with the corresponding results obtained for three-dimensional rods. The effective stiffness properties in [2] are expressed as a combination of material parameters and geometry of layers.

We consider now a static three-dimensional Cosserat beam made of homogeneous material [4]. The matrices of elasticity coefficients of the beam are defined as follow:

$$\mathbf{C}^{\Gamma} := \mathrm{Diag}\,(GA\ GA\ EA) \quad \text{and} \quad \mathbf{C}^{K} := \mathrm{Diag}\,(EI\ EI\ GJ) \tag{1}$$

where A is the cross-sectional area of the rod, I is the principal moment of inertia of the circular cross-section, $J = 2I$ is the polar moment of inertia, E is Young's modulus, $G = E/[2(1+\nu)]$ is the shear modulus, and ν is Poisson's ratio. For homogenization purposes, the new effective stiffness properties are used as inputs in the stiffness matrices in (1).

Maximum deflection and rotation are evaluated by using analytical approach for benchmark problems for the directed curves in [2]. Those results are compared to the numerical ones obtained from the geometrically exact beam model using the homogenized effective stiffness coefficients. In case of a cantilever beam undergoing point force at the free end, the comparison in Fig. 2 shows that for small loads results in terms of deflections are the same, while increasing the load magnitude, results in the linear and nonlinear frames diverge. In case of pure torsion applied at the free end of a cantilever beam, results in the linear and nonlinear theories match, see Fig. 3. Analyses are carried out for different configurations of cross-section.

As a conclusion, this work represents a comparison of the linear model from [2] and a nonlinear Cosserat beam model for the case of multi-material layered cross-sections. This process is useful to study more complex inhomogeneous cross-section models, in particular in case of unloaded shaft of endoscopes. The characterisation of

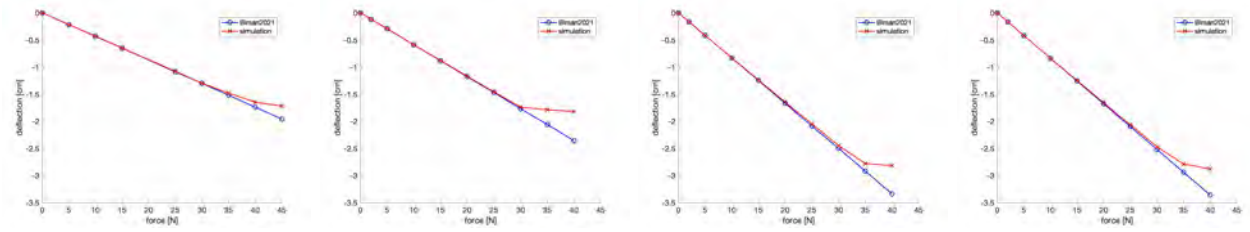

(a) (b) (c) (d)

Figure 2: Deflection of a cantilever undergoing point force at the free end: (a) steel core and face, (b) aluminium core and steel face, (c) polypropylen core and steel face, (d) empty core and steel face.

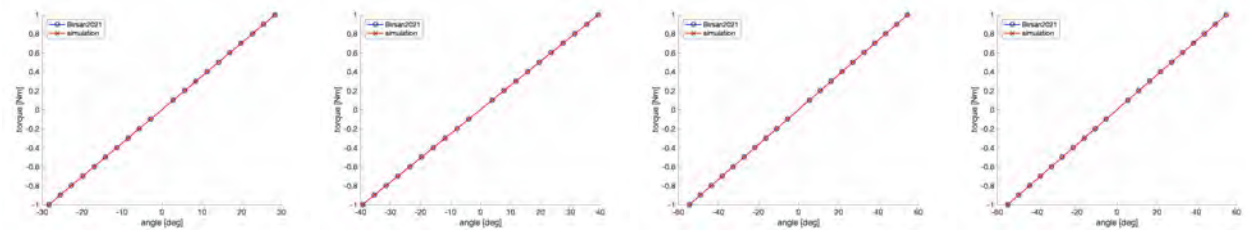

(a) (b) (c) (d)

Figure 3: Torsion of a cantilever undergoing point force at the free end: (a) steel core and face, (b) aluminium core and steel face, (c) polypropylen core and steel face, (d) empty core and steel face.

the effective properties for inhomogeneous cross-sections will be validated through experimental campaigns.

Acknowledgments

This project has received funding from the European Union's Horizon 2020 research and innovation under the Marie Skłodowska-Curie grant agreement No.860124.

References

[1] U. K. Chakravarty. On the modeling of composite beam cross-sections. Elsevier, Composites Part B: Engineering, 42(4):982-991, 2011

[2] M. Birsan, D. Pietras, T. Sadowski. Determination of effective stiffness properties of multilayered composite beams. Continuum Mechanics and Thermodynamics, 1-23, 2021

[3] M. Birsan, H. Altenbach, T. Sadowski. et al.. Deformation analysis of functionally graded beams by the direct approach. Composites Part B: Engineering, 43(3):1315-1328, 2012

[4] S. Leyendecker, P. Betsch, P. Steinmann. Objective energy-momentum conserving integration for the constrained dynamics of geometrically exact beams. Computer Methods in Applied Mechanics and Engineering, 195(19-22):2313-2333, 2006

Numerical convergence order study of mixed order variational integrators

Theresa Wenger, Sina Ober-Blöbaum, Sigrid Leyendecker

The simulation of mechanical systems that act on multiple time scales is challenging. For resolving the fast motion a tiny time step is required, whereas for the slow motion a coarser approximation is accurate enough, pointing out the conflict of highly accurate results versus low computational costs. Typical examples of systems comprising dynamics on different time scales can be found in astrophysics, molecular dynamics, and vehicle dynamics, to mention just a few.
It is assumed that the potential of the mechanical system is composed of different parts with strongly varying dynamics acting on different time scales, and thus, to be separable into a slow potential V and a fast potential W. Furthermore, the configuration variable might be split into slow and fast variables.
The derivation of the mixed order variational integrators bases on a discrete version of Hamilton's principle. Polynomials of possibly different degrees are considered for the approximation of the slow and fast degrees of freedom together with possibly different quadrature rules of appropriate order to approximate the contributions of the action. Due to their variational derivation, the integrators preserve the underlying geometric structure of the system as momentum maps and symplecticity.
We focus here on integrators based on a f order polynomial for the approximation of the configuration together with the symmetric trapezoidal rule for the integral approximation of the slow potential and a Gauss quadrature of order $2f$ for the integral approximation of the fast potential. The choice $f = 1$ together with the Gauss quadrature of order two, i.e. the midpoint rule, yields an integrator equivalent to the IMEX method presented in [SG09]. The integrators can be interpreted as impulse methods with an explicit kick of the slow force, updating the fast motion implicitly, and an explicit kick of the slow force in the end. If the fast potential is quadratic, the presented integrators are fully explicit independent of the choice of f.
The Fermi-Pasta-Ulam problem (FPU) is a nontrivial highly oscillatory conservative system. Due to its rich multiscale coupling behaviour, the FPU is a popular test problem for numerical integrators. It consists of 2ℓ masses linked with alternating weak cubic and stiff linear springs. The Lagrangian contains a slow potential and a quadratic fast potential reading

$$\begin{aligned} L(q,\dot{q}) =& \frac{1}{2}\sum_{i=1}^{l}(\dot{q}_i^s)^2 + \frac{1}{2}\sum_{i=1}^{l}(\dot{q}_i^f)^2 \\ & - \frac{1}{4}\left[(q_1^s - q_1^f)^4 + \sum_{i=1}^{\ell-1}(q_{i+1}^s - q_{i+1}^f - q_i^s - q_i^f)^4 + (q_l^s + q_l^f)^4\right] - \frac{\omega^2}{2}\sum_{i=1}^{\ell}(q_i^f)^2 \end{aligned} \tag{1}$$

with $\omega \gg 1$. The variable q_i^s represents the location of the centre of the i-th stiff spring and the variable q_i^f its length, $i = 1, \dots, l$. The third term in equation (1) is the soft spring potential V depending on the complete configuration variable, while the fourth term is the stiff potential $W(q^f)$ depending on the spring lengths only. The vibration of the stiff linear springs takes place on the time scale ω^{-1}, while ω^0 is the time scale of the soft nonlinear springs' motion [HLW06].
Six masses are included in the simulations, i.e. three stiff springs. The simulation time is set to $t_N = 1$ and the stiffness ω to 50. The convergence order of the integrators is analysed numerically. The simulation results calculated by the Störmer-Verlet method with time step $h = 10^{-6}$ serve as a reference to determine the maximum global errors in the configurations q^s and q^f. The convergence orders of the integrators are shown in Figure 1. The evolution of the errors in q^s and q^f dependent on the time step sizes h are depicted. It can be seen that the error in the slow configuration converges with order two for all choices of f. The errors in q^s nearly lay on top of each other. Looking at the errors in q^f the convergence order for $f = 1$ is two, whereas for $f = 2, \dots, 5$ the errors converge in the beginning with an order higher than two. In particular for $f = 2$ it is possible to determine the convergence order to be of approximate four. When the time steps get smaller, the slope changes to two. The errors in q^f have the same magnitudes as their slow counterparts now. It seems as if the error in q^f is dominated now by the error in q^s. This can be explained by the coupling potential V. When the convergence order reduces, the error in q^s starts to influence the approximations of q^f through V and eventually dominates. Note that for $f = 1$ the error in q^f is larger than for $f = 2, \dots, 5$ and, furthermore, the error in the fast components are always higher than in the slow ones.
When increasing f, only the propagation matrix for the explicit update of the fast oscillations changes. Therefore, increasing f is not accompanied by an increased runtime. Thus, an improvement in the accuracy of the

fast variable can be achieved without any additional costs by choosing $f > 1$, see Figure 2, where the errors in q^s (left) and q^f (right) are plotted over the runtime.

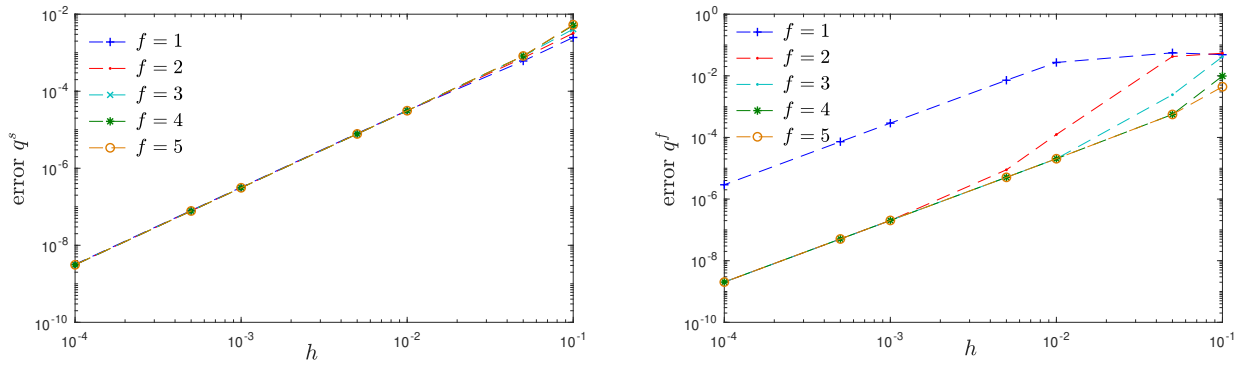

Figure 1: FPU: Global errors of the slow configurations q^s (left) and fast configurations q^f (right) versus time step size h for $s = 1, \ldots, 5$ ($\omega = 50$)

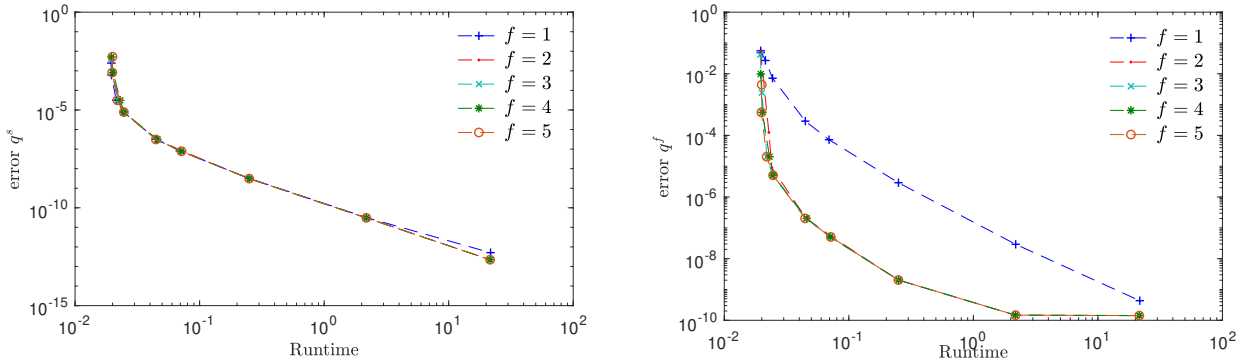

Figure 2: FPU: Global errors of the slow configurations q^s (left) and fast configurations q^f (right) versus runtime for $s = 1, \ldots, 5$ ($\omega = 50$)

References

[HLW06] Ernst Hairer, Christian Lubich, and Gerhard Wanner. *Geometric numerical integration: structure-preserving algorithms for ordinary differential equations*, volume 31 of *Springer Series in Computational Mathematics*. Springer, Berlin Heidelberg, 2006.

[SG09] A. Stern and E. Grinspun. Implicit-explicit variational integration of highly oscillatory problems. *SIAM Multiscale Modeling and Simulation*, 7(4):1779–1794, 2009.

4 Activities

4.1 Improved organization of IT systems

Logins at shared computers are now based on IdM and FAU's Microsoft Active Directory (FAUAD). This holds not only for the Windows machines in the labs but also for the macOS machines in the student CIP pool, as well as all Linux machines at the institute.
A web service called `ltd-monitor` provides a database with web API for storing information about users, rooms, computers, research projects, etc. A browser-based user interface shows an overview of all lab and CIP computers, including their online status, and an option to wake up machines for remote use. The web service also generates up-to-date configuration files for the network routers, the DHCP server, and the DNS, avoiding double bookkeeping of administrative data.
Git together with a self-hosted GitLab instance is increasingly used for text-based development tasks. Next to individual use, the development of teaching material is now done mostly via GitLab. This change provided an opportunity to clan up long-lived LaTeX projects. GitLab's CI/CD feature is now used to run automated tests which help to maintain clean projects and give contributors immediate machine-generated feedback in case of obvious problems. Further, automated server-side compilation of the LaTeX documents ensures that all contributions compile without errors inside a fresh Linux container.
On macOS and Linux (and Windows via Windows Subsystem for Linux), all users are invited to use a common set of configuration files which facilitate command-line based workflows.

4.2 Teaching during Covid-19 pandemic

In 2021 the Covid-19 pandemic is still present. During the summer semester the lectures at LTD were held online and received very sucessful reviews, in particular "Statik und Festigkeitslehre", which relied on "live-streaming"; this modality played an important role in the students' engagement.
By the end of the summer, a good percentage of FAU students and staff was already vaccinated against the virus. Therefore, for the winter semester, FAU decided to return to the lecture halls, starting with a 3G rule (recovered, vaccinated or tested). Later on, FAU was the first university in Germany to follow a strict 2G guideline for the lectures on campus (vaccinated or recovered).
LTD continued with offering all lectures in a hybrid model, both in presence and recorded videos.

4.3 Motion capture laboratory

Our motion analysis lab is equipped with a camera and marker based optical tracking system, including 10 Qualisys MoCap high speed cameras and 2 Qualisys high speed video cameras, as well as Noraxon MyoMotion inertial sensors, Cybergloves III to measure hand joint angle kinematics, force plates, and Noraxon Desktop DTS electromyography sensors.

A frame was constructed to bring the cameras closer to the markers in order to perform motion capturing for small human actions, such as motion of hand digits. With this setup, kinematic parameter identification for joints in the human hand, especially the wrist, the metacarpophalangeal and interpalangeal joints has been performed. This is an essential first step towards formulating a procedure for effective parameter identification to setup subject-specific models. This will enable us to perform biomechanical optimal control simulations with higher levels of confidence and use the results as measures of human performance.

The motion capture laboratory increased its performance by taking a step forward with the measurement of patients in cooperation with the Department of Medicine 3 - Rheumatology and Immunology of the Universitätsklinikum Erlangen. Some of these collaborations include

- CyberGlove: The analysis of hand movements can yield useful information and indicators for the detection of rheumatic diseases at an early stage. The CyberGlove project goal is to analyze whether the glove bears potential for this purpose. In a second step, we aim to measure activities of daily life and examine if the use of specific joints has an impact on the development of arthritis.
- Developement of pilot projects

4.4 Dynamic laboratory

The dynamic laboratory – modeling, simulation and experiment (Praktikum Technische Dynamik) adresses all students of the Technical Faculty of the Friedrich-Alexander-Universität Erlangen-Nürnberg. The aim of the practical course is to develop mathematical models of fundamental dynamical systems to simulate them numerically and compare the results to measurements from the real mechanical system. Here, the students learn

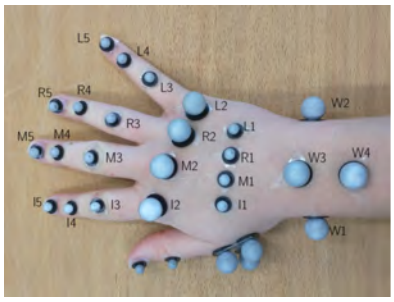

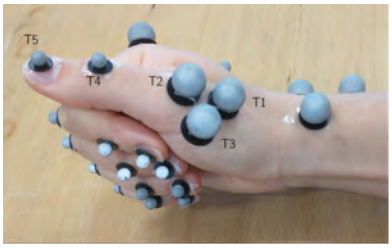

both the enormous possibilities of computer based modeling and its limitations. The course contains one central programming exercise and six experiments observing various physical phenomena along with corresponding numerical simulations:

- programming exercise
- beating pendulums
- gyroscope
- ball balancer system
- robot arm
- inverse pendulum
- balancing robot

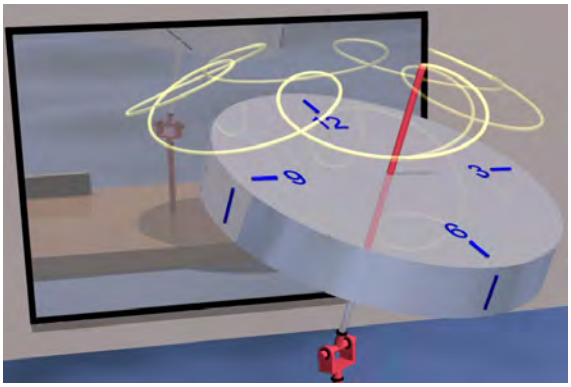

programming exercise

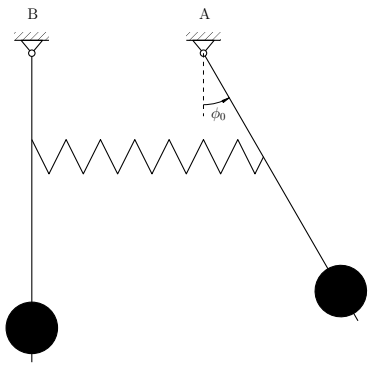

beating pendulums

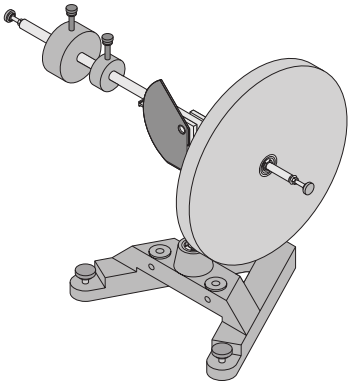

gyroscope

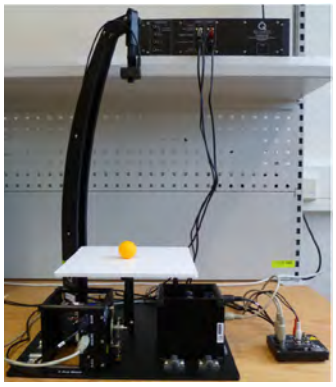

ball balancer system

robot arm

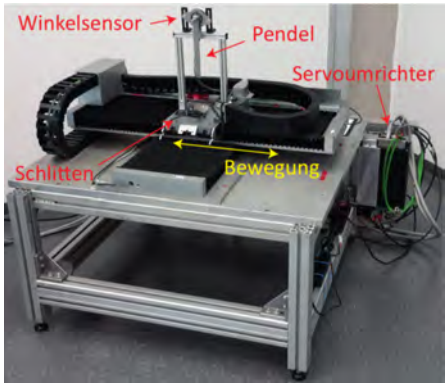

inverse pendulum

balancing robot

4.5 MATLAB laboratory

The MATLAB laboratory (Praktikum MATLAB) is offered to all students of the Technical Faculty of the Friedrich-Alexander-Universität Erlangen-Nürnberg. The course aims to teach the participants the basic skills of numerical programming in MATLAB. The course is offered in conjunction with the Institute of Applied Mechanics (LTM), the Institute of Production Metrology (FMT) and the Institute of Engineering Design (KTmfk). The first lecture is an introductory programming session for MATLAB fundamentals. Thereafter, every institute presents a task related to mechanics and engineering, for example, the LTD task is to understand and simulate, the dynamics of a crane. The task is introduced to the students through a theory lecture, which is then followed by programming sessions.

4.6 THREAD - Geometric numerical integration, Young Researchers Minisymposium

The minisymposium was organized by M.Sc. Andrea Leone, M.Sc. Ergys Çokaj and M.Sc. Martina Stavole (Marie Curie Fellows at THREAD network) in cooperation with Prof. Dr.-Ing. habil. Sigrid Leyendecker at the Conference on the Numerical Solution of Differential and Differential-Algebraic Equations (NUMDIFF-16).

4.7 Teaching

Winter semester 2021/2022

Dynamik starrer Körper (MB, ME, WING, IP, BPT, CE, MT)		
Vorlesung		S. Leyendecker
Übung + Tutorium		T. Wenger, D. Holz D. Martonová, G. Capobianco
Mehrkörperdynamik (MB, ME, WING, TM, BPT, MT)		
Vorlesung		S. Leyendecker
Übung		T. Wenger
Praktikum Technische Dynamik – Modellierung, Simulation und Experiment (MB, ME, WING)		S. Leyendecker D. Holz, R.T. Sato Martín de Almagro M. Schubert, G. Capobianco
Praktikum Matlab (MB)		S. Leyendecker M. Schubert

Summer semester 2021

Biomechanik (MT)		
Vorlesung + Übung		S. Budday
geprüft	48 + 9 (WS 2020/2021)	
Geometric numerical integration (MB, ME, WING, BPT)		
Vorlesung		S. Leyendecker R.T. Sato Martín de Almagro
Übung		E.S. Scheiterer
geprüft	4 + 0 (WS 2020/2021)	
Statik und Festigkeitslehre (BPT, CE, ME, MWT, MT)		
Vorlesung		S. Leyendecker
Tutorium		D. Holz, D. Martonová J. Penner, U. Phutane
Übung		D. Holz, D. Martonová R.T. Sato Martín de Almagro
geprüft	257 + 237 (WS 2020/2021)	
Praktikum Matlab (MB)		
Teilnehmer	61	S. Leyendecker T. Wenger, E. Schaller M. Franz, A. Müller

Winter semester 2020/2021

Dynamik starrer Körper (MB, ME, WING, IP, BPT, CE, MT)

Vorlesung		S. Leyendecker
Tutorium		D. Holz, H. Lang D. Martonová, J. Penner T. Wenger
Übung		D. Holz, M. Klebl U. Phutane
geprüft	310 + 85 (SS 2021)	

Mehrkörperdynamik (MB, ME, WING, TM, BPT, MT)

Vorlesung		S. Leyendecker
Übung		J. Penner
geprüft	76 + 17 (SS 2021)	

Geometric beam theory (MB, ME, WING, BPT)

Vorlesung + Übung		S. Leyendecker R.T. Sato Martín de Almagro

Praktikum Technische Dynamik – Modellierung, Simulation und Experiment (MB, ME, WING)

Teilnehmer	10	S. Leyendecker D. Holz, M. Klebl D. Martonová, J. Penner U. Phutane

Praktikum Matlab (MB)

Teilnehmer	67	S. Leyendecker, U. Phutane E. Schaller, A. Müller, M. Franz

4.8 Theses

Master theses

- Matthias Schubert
  Optimal control simulations of geometrically exact beam dynamics via the discrete adjoint method
- Simon Heinrich
  On the personalization of kinematic human hand models

Project theses

- Simon Heinrich
  Lower body joint angle determination during human gait based on optical segment positioning using CGM2.4 and marker clusters
- Marc Gadinger
  Optimal control of a ball-balancer system

Bachelor theses

- Dorothea Brackenhammer
  Finite-Elemente-Modellierung: Erste Schritte zur Entwicklung mechanischer Unterstützung eines von der Kardiomyopathie betroffenen Herzens
- Dardan Bersisha
  Auswertung biomechanischer Messungen der menschlichen Hand zur Analyse von funktionalen Bewegungseinschränkungen

4.9 Seminar for mechanics

together with the Chair of Applied Mechanics LTM

09.11.2021 M.Sc. Ajay Kumar Pasupuleti
Universität Duisburg-Essen
Towards phase field modelling using the scaled boundary finite element method

02.06.2021 M.Sc. Andrea Leone
Department of Mathematical Sciences
Norwegian University of Science and Technology
Lie group integrators approach for a multibody system

02.06.2021 M.Sc Ergys Çokaj
Department of Mathematical Sciences
Norwegian University of Science and Technology
Dynamics of the n-fold pendulum in the frameworkof Lie group integrators

01.06.2021 M.Sc. Giuseppe Capobianco
Institut für Nichtlineare Mechanik,
Universität Stuttgart
Mechanical systems with frictional contact: Geometric theory and numerical simulation

4.10 Editorial activities

Advisory and editorial board memberships Since January 2014, Prof. Dr.-Ing. habil. Sigrid Leyendecker is a member of the advisory board of the scientific journal Multibody System Dynamics, Springer. She is a member of the Editorial Board of ZAMM – Journal of Applied Mathematics and Mechanics / Zeitschrift für Angewandte Mathematik und Mechanik since January 2016 and since 2017 runs a second term as member of the managing board of the International Association of Applied Mathematics and Mechanics (GAMM), as well as a member of the executive council of the German Association for Computational Mechanics (GACM) and member of the General Council of the International Association for Computational Mechanics (IACM).

Since October 2017, Prof. Dr.-Ing. habil. Sigrid Leyendecker is an elected member of the Faculty Council of the Faculty of Engineering at the Friedrich-Alexander-Universität Erlangen-Nürnberg, and in April 2019 was elected deputy Chair of the Qualification Assessment Committee (Eignungsfeststellungsverfahrens-(EFV-)Kommission) of the Bachelor's degree programme Medical Engineering, at the Friedrich-Alexander-Universität Erlangen-Nürnberg.

5 Publications

5.1 Reviewed journal publications

1. D. Huang and S. Leyendecker. "An electromechanically coupled beam model for dielectric elastomer actuators". *Computational Mechanics*, DOI 10.1007/s00466-021-02115-0, 2021

2. M. Lohmayer, P. Kotyczka and S. Leyendecker. "Exergetic Port-Hamiltonian Systems: Modelling Basics". *Mathematical and Computer Modelling of Dynamical Systems*, Vol. 27, pp. 489-521, DOI 10.1080/13873954.2021.1979592, 2021

3. D. Holz, M.T. Duong, D. Martonová, M. Alkassar and S. Leyendecker. "A Transmural Path Model Improves The Definition of The Orthotropic Tissue Structure in Heart Simulations". *Journal of Biomechanical Engineering*. Vol. 144(3), pp. 031002, DOI doi.org/10.1115/1.4052219, 2021.

4. D. Martonová, M. Alkassar, J. Seufert, D. Holz, M.T. Duong, B. Reischl, O. Friedrich and S. Leyendecker. "Passive mechanical properties in healthy and infarcted rat left ventricle characterised via a mixture model". *Journal of the Mechanical Behavior of Biomedical Materials*, Vol. 119(104430), DOI 10.1016/j.jmbbm.2021.104430, 2021.

5. U. Phutane, A. M. Liphardt, J. Bräunig, J. Penner, M. Klebl, K. Tascilar, M. Vossiek, A. Kleyer, G. Schett, and S. Leyendecker. "Evaluation of Optical and Radar Based Motion Capturing Technologies for Characterizing Hand Movement in Rheumatoid Arthritis — A Pilot Study". *Sensors*, Vol. 21(4), pp. 1208, DOI 10.3390/s21041208, 2021.

6. D. Martonová, D. Holz, M.T. Duong and S. Leyendecker. "Towards the simulation of active cardiac mechanics using a smoothed finite element method". *Journal of Biomechanics*, Vol. 115, pp. 110153, DOI 10.1016/j.jbiomech.2020.110153, 2021.

7. T. Leitz, R.T. Sato Martín de Almagro and S. Leyendecker. "Multisymplectic Galerkin Lie group variational integrators for geometrically exact beam dynamics based on unit dual quaternion interpolation — no shear locking". *Computer Methods in Applied Mechanics and Engineering*, Vol. 374, pp. 113475, DOI 10.1016/j.cma.2020.113475, 2021.

5.2 Invited lectures

1. S. Leyendecker, J. Penner and U. Phutane. "Geometric numerical integration in simulation and optimal control of biomechanical motion", invited lecture, *GAMM Annual Meeting*, Kassel, Germany 15-19 March 2021.

5.3 Conferences and proceedings

1. X. Chen, S. Leyendecker and H. van den Bedem. "SARS Covid-19 main protease mutation analysis by the kinematic method". *ECCOMAS Thematic Conference on Multibody Dynamics*, Budapest, Hungary 12-15 December 2021.

2. J. Michaelis, I. Reiher, S. Heinrich, B. Coppers, G. Schett, A. Kleyer, D. Elewaut, M. De Craemer, S. Leyendecker and A.M. Liphardt. "CyberGlove for clinical use?", *FAU-Networking Night Medizintechnik*, Erlangen, 27 October 2021.

3. D. Phansalkar, K. Weinberg, M. Ortiz and S. Leyendecker, "Dynamic simulation of a phase-field fracture with the Newmark method". *6th Research Training Group GRK 2423 FRASCAL*,Neuhof an der Zenn, 14-16 October 2021.
4. D. Holz, M.T. Duong, D. Martonová, M. Alkassar and S. Leyendecker. "Discontinuous Galerkin-based approach to define orthotropic tissue structure in computational heart models". *International Conference on Computational Biomechanics*, Paris, France, 20-21 September 2021.
5. M. Lohmayer, P. Kotyczka and S. Leyendecker. "GENERIC and Port-Hamiltonian structures for complex systems", *Joint European Thermodynamics Conference*, Prague, Czech Republic, 14-18 June 2021.
6. R.T. Sato Martín de Almagro. "High-order integrators on homogeneous spaces via nonholonomic mechanics". In: *Proceedings of the Conference on the Numerical Solution of Differential and Differential-Algebraic Equations*, *NUMDIFF-16*, 2021.
7. D. Phansalkar, K. Weinberg, M. Ortiz and S. Leyendecker. "Uniform and adaptive in phase-field models for brittle fractures". *5th Research Training Group GRK 2423 FRASCAL*, online 30 April 2021.
8. E.S. Scheiterer and S. Leyendecker. "Forward dynamics simulation of a human leg model with a geometrically exact beam model as prosthetic foot". In: *Proc. Appl. Math. Mech.*,*PAMM*, DOI: 10.1002/pamm.202100096, 2021.
9. D. Martonová, M. Alkassar, J. Seufert, D. Holz, M.T. Duong, B. Reischl, O. Friedrich and S. Leyendecker. "Influence of passive mechanical properties in healthy and infarcted rat myocardium on the cardiac cycle". In: *Proc. Appl. Math. Mech.*,*PAMM*, DOI: 10.1002/pamm.202100054, 2021.
10. X. Chen, S. Leyendecker and H. van den Bedem. "Vibrational entropy calculation of proteins via kinematic flexibility analysis". *GAMM Annual Meeting*, Kassel, Germany 15-19 March 2021.
11. T. Leitz, R.T. Sato Martín de Almagro and S. Leyendecker. "Galerkin variational integration of the geometrically exact beam via unit dual quaternion interpolation". *GAMM Annual Meeting*, Kassel, Germany 15-19 March 2021.
12. D. Phansalkar, K. Weinberg, M. Ortiz and S. Leyendecker. "Space-dependent transition zone parameter for a phase-field model of brittle fractures". *GAMM Annual Meeting*, Kassel, Germany 15-19 March 2021.
13. E.S. Scheiterer and Leyendecker. "Fuzzy forward dynamics of a human leg with a prosthetic foot". *GAMM Annual Meeting*, Kassel, Germany 15-19 March 2021.
14. D. Martonová, M. Alkassar, J. Seufert, D. Holz, M.T. Duong, B. Reischl, O. Friedrich and S. Leyendecker. "Characterisation of passive mechanical properties in healthy and infarcted rat myocardium". *GAMM Annual Meeting*, Kassel, Germany 15-19 March 2021.
15. M. Stavole, T. Wenger and S. Leyendecker. "Variational formulation and simulation of the 1D wave equation and geometrically exact beam dynamics". *MaGIC 2021: Workshop on Manifolds and Geometric integration*, Bergen and Trondheim, Norway 1-5 March 2021.
16. E.S. Scheiterer and S. Leyendecker. "Predeformed geometrically exact beam model for a dynamic-response prosthesis". In: *Proc. Appl. Math. Mech.*,*PAMM*, DOI:10.1002/pamm.202000152, 2021.
17. D. Huang and S. Leyendecker. "Modelling of Electromechanical Coupling in Geometrically Exact Beam Dynamics". In: *Proceedings of the 14th WCCM-ECCOMAS Congress 2020* DOI: 10.23967/wccm-eccomas.2020.207, 2021.

6 Social events

In 2021 most of the social activities were still restricted due to the Covid-19 pandemic.

Farewell of team members

Hosting of THREAD secondments

LTD hosted ESR Andrea Leone and ESR Ergys Çokaj for one month to work on discrete mechanics of beams.